CONTROLS ON CYCLOSTRATIGRAPHY OF LOWER CRETACEOUS CARBONATES AND EVAPORITES, CUPIDO AND COAHUILA PLATFORMS, NORTHEASTERN MEXICO

CHRISTOPH LEHMANN[1*], DAVID A. OSLEGER[2], AND ISABEL P. MONTAÑEZ[2]

[1] *Department of Earth Sciences, University of California, Riverside, California 92521, U.S.A.*

[2] *Department of Geology, University of California, Davis, California 95616, U.S.A.*

**Present address: Amoco Exploration and Production, 501 WestLake Park Boulevard, Houston, Texas 77079-2696, U.S.A.*

ABSTRACT: **The Lower Cretaceous Cupido (Barremian–Aptian) and Coahuila (Albian) carbonate platforms of northeastern Mexico exhibit thick successions of meter-scale cycles deposited in three unique paleoenvironmental settings. (1) The Cupido shelf lagoon is composed of peritidal carbonate cycles deposited in the protected lee of a reef-rimmed to barrier-shoal margin. (2) The restricted Coahuila ramp interior consists of cyclic alternations of subtidal evaporites and peritidal carbonates. (3) The deep-water parts of both the Cupido and Coahuila platforms are composed of foraminiferal wackestones and lime mudstones interspersed with firmgrounds and hardgrounds in a ''cyclic'' arrangement. Vertical successions of meter-scale evaporitic cycles and peritidal cycles exhibit systematic stacking patterns that build into intermediate-scale high-frequency sequences (tens to hundreds of meters thick), and large-scale composite sequences (hundreds of meters thick) that can be correlated across the Cupido and Coahuila platforms. These large-scale stacking patterns are interpreted to reflect long-term accommodation events and, when combined with the scale-independent architecture of all genetic units, permit the inference that all three meter-scale cycle types on the Cupido and Coahuila platforms are also governed by relative sea-level change.**

The composition, thickness, and number of meter-scale cycles within individual high-frequency sequences can be highly variable across the Cupido and Coahuila platforms, however, even though the overall upward-shallowing patterns are evident. The lateral complexity of cycle architecture and distribution is interpreted to be a natural response to fluctuations in regional climate interacting with autogenic processes such as variations in carbonate production and dispersal, intensity and frequency of tropical storms and monsoons, thermohaline circulation patterns, and ambient ocean chemistry and temperature. These interacting processes created laterally variable physiographic and oceanographic conditions across the Cupido and Coahuila platforms, complicating the sedimentary record generated by the composite sea-level signal.

Well-documented evidence from Barremian–Cenomanian pelagic cycles throughout the Tethyan seaway strongly indicates that Milankovitch-driven climatic changes operated during the Early Cretaceous. Contemporaneous shallow-marine cyclicity in several locations suggests that these climatic changes may have had globally widespread effects. In an effort to link the shallow-water and deep-water realms, we propose a model whereby Milankovitch-driven global climatic changes generated low-amplitude, high-frequency eustatic fluctuations through some combination of thermal expansion and contraction of ocean water, waxing and waning of small ice caps and alpine glaciers, and changes in the storage capacity of aquifers and lakes to produce meter-scale cycles across Lower Cretaceous shallow-marine platforms.

INTRODUCTION

Cretaceous stratigraphic cyclicity is recorded in a variety of depositional and tectonic settings, from pelagic settings (e.g., de Boer 1982; Herbert and Fischer 1986; Park and Oglesby 1991), foreland basins (e.g., Kauffman 1977; Elder et al. 1994; Sethi and Leithold 1994; Sageman et al. 1997), and shallow carbonate platforms (e.g., Minero 1988; Strasser 1988; Goldhammer et al. 1991; Grötsch 1996; Röhl and Ogg 1996). The mechanisms behind development of Cretaceous deep-water cycles have commonly been linked to climatic changes driven by orbital variations in the Milankovitch frequency band. These climatic changes generated variations in ocean-surface productivity, ocean-bottom redox conditions, thermohaline circulation patterns, and nutrient flux from the continents. In contrast, most cyclostratigraphic studies of Cretaceous shallow-marine successions suggest that the prevailing control on stratigraphic cyclicity is eustasy, perhaps in concert with regional climate change. Consequently, Cretaceous deep-water and shallow-water settings have been viewed as decoupled systems, a perspective that seems unlikely given the connections apparent in today's oceans.

The Lower Cretaceous Cupido and Coahuila carbonate platforms of northeastern Mexico (Fig. 1) exhibit meter-scale cycles deposited in three distinct paleoenvironmental settings: restricted evaporitic lagoon, peritidal shelf-lagoon, and low-energy deep platform. The intent of this paper is to (1) illustrate the various architectural arrangements of lithofacies within meter-scale cycles of the Cupido and Coahuila platforms, (2) evaluate potential controls to determine if the three cycle types were generated by processes unique to their depositional settings, or whether these cycles were formed by a single common mechanism, and (3) compare these shallow-marine cycles from northeastern Mexico with coeval Cretaceous deep-water cycles from elsewhere in the Tethyan seaway to assess potential connections and larger-scale controlling mechanisms.

PREVIOUS WORK AND METHODS

Regionally comprehensive sedimentologic or sequence stratigraphic studies have not been undertaken on the Cupido and Coahuila carbonate platforms since the component formations were originally described in lithostratigraphic and biostratigraphic terms (Burrows 1909; Böse 1927; Imlay 1936, 1937, 1938, 1944a, 1944b; Kelly 1936; Kellum et al. 1936; Humphrey 1949; Humphrey and Diaz 1956, unpublished work). More recent investigations have focused on individual parts of the platforms exposed in isolated mountain ranges in the area (de Cserna 1956; Fuentes 1964; Krutak 1967; Bishop 1970; Bloxsom 1972; Garza 1973; Charleston 1974; Wilbert 1976; Conklin and Moore 1977; Wilson and Pialli 1977; Longoria and Gamper 1977; Elliot 1979; Ross 1981; Longoria 1984; Wilson et al. 1984; Tinker 1985; Cantú Chapa et al. 1985; Kindred 1988; Cantwell and Ward 1990; Longoria and Monreal 1991; Morán- Zenteno 1994). Recently, a broad-scale sequence stratigraphic framework was proposed by Goldhammer et al. (1991) for the upper part of the Cupido Formation and Wilson and Ward (1993) synthesized large-scale depositional patterns of the Cupido and Coahuila carbonate platforms, as well as coeval platforms of east-central Mexico.

In this study, 37 sections totaling 17,000 m were logged on a decimeter scale throughout the $> 80{,}000$ km^2 study area (Fig. 2). Sections composed of evaporitic interior facies, shallow shelf-lagoon facies, and high-energy shoal-margin facies were measured on the Coahuila block (including the Sierra de la Peña), in the northern part of the Sierra de Parras, and in the Sierra de Jimulco. Sections composed of deep-platform facies were measured in the southern part of the Sierra de Parras, in the eastern Sierra Madre Oriental, and in isolated mountain ranges east and north of the Sierra de Paila. Hand samples were collected at 10–20 m intervals at selected platform-margin and platform-interior sections and at 5–10 m intervals at

JOURNAL OF SEDIMENTARY RESEARCH, VOL. 68, NO. 6, NOVEMBER, 1998, P. 1109–1130
 1073-130X/98/068-1109/$03.00

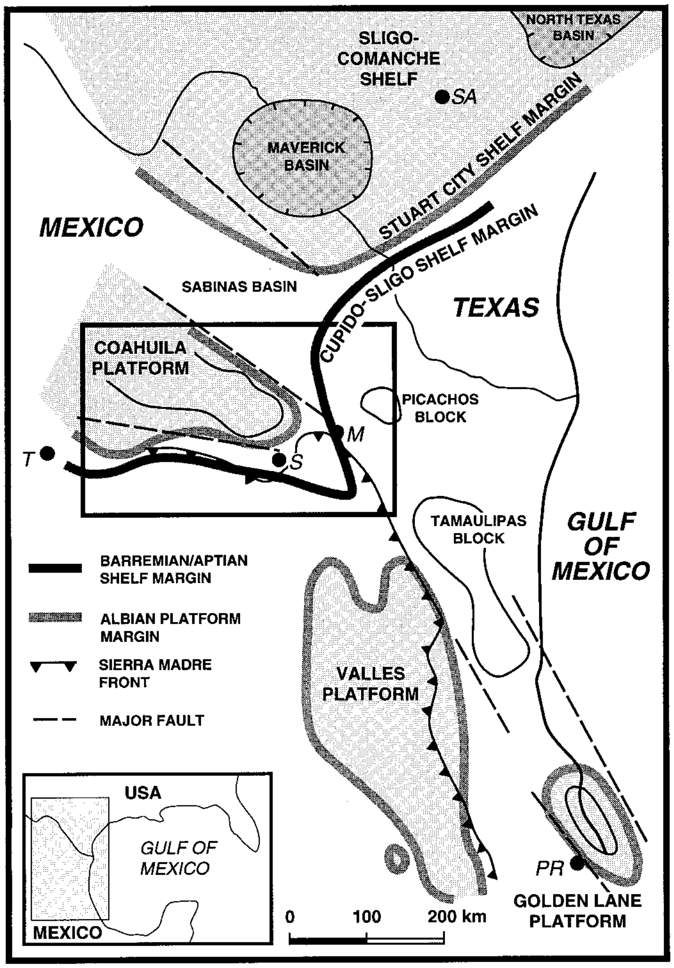

FIG. 1.—Tectonic map of northeastern Mexico showing distribution of Barremian–Aptian and Aptian–Albian carbonate platforms (modified after Wilson and Ward 1993). Shaded areas are for the Albian platforms only. Solid thin line within Coahuila platform is interpreted edge of Permo-Triassic granodioritic basement (Coahuila block). Rectangle outlines the study area. M = Monterrey, S = Saltillo, T = Torreon, PR = Poza Rica, SA = San Antonio.

selected deep-platform sections for petrographic study of individual lithofacies.

TECTONIC, STRATIGRAPHIC, AND CLIMATIC SETTING

The Cupido and Coahuila carbonate platforms of northeastern Mexico were part of an extensive carbonate system that rimmed the ancestral Gulf of Mexico during the Early Cretaceous. These two platforms span Barremian through Albian time and are contemporaneous with the Sligo and Comanche shelves in Texas and the Valles and Golden Lane platforms in Mexico (Fig. 1; Wilson 1975). The Barremian to early Aptian Cupido shallow-marine shelf developed around the emergent Coahuila granodioritic and metasedimentary basement block, which formed after early Mesozoic rifting (Winker and Buffler 1988; Wilson 1990; Wilson and Ward 1993) (Figs. 3, 4A). Subsequent deepening during the early to mid-Aptian led to the retrograde backstep of the Cupido platform and eventual shallow-marine deposition on the Coahuila block (Fig. 3; Lehmann 1997). Peak flooding during the mid- to late Aptian is marked by the deposition of argillaceous carbonates and shales of the La Peña Formation.

The Albian Coahuila inner ramp and ramp crest developed on top of and around the Coahuila block, a position reflecting significant backstep from the Barremian to Aptian Cupido shelf margin (Figs. 3, 4B). Evaporites and carbonates of the Acatita Formation were deposited in the restricted interior of the ramp, while the time-equivalent Upper Tamaulipas Formation was deposited in deeper parts of the outer ramp. Albian shallow-subtidal carbonates of the Aurora Formation form the ramp-crest barrier and ultimately bury Acatita mixed evaporites and carbonates (Fig. 3). The Coahuila platform was flooded and ultimately drowned during latest Albian and Cenomanian time with the deposition of hemipelagic mudstones and deep-water laminites of the Sombreretillo and Cuesta del Cura Formations. The termination of shallow-marine carbonate deposition on the Coahuila platform likely corresponds with the worldwide drowning of carbonate platforms during the *Rotalipora appenninica* time interval (Grötsch et al. 1993; Vahrenkamp et al. 1993; Sliter 1995; Lehmann 1997).

The Cupido and Coahuila carbonate platforms developed during peak Cretaceous greenhouse climatic conditions (Barron 1983). Regionally, evaporites and sabkha carbonates of the Cupido and Coahuila platforms indicate arid to semiarid conditions in northeastern Mexico from Barremian to Albian time. Coeval evaporites are common around the northwestern Gulf of Mexico (e.g., the La Virgen of the Sabinas basin, the Ferry Lake of the northern Gulf coast, the Kirschberg of the Comanche shelf, the McKnight of the Maverick basin, as well as evaporites deposited in the interior of the Valles and Golden Lane platforms; Wilson and Ward 1993; McFarlan and Menes 1991).

The latitudinal temperature gradient in the oceans was flat during the Cretaceous (Barron 1983); presumably high ocean-water temperatures characterized the poles, and the water column was stratified. Evidence for warm temperatures in the Cretaceous oceans has been determined from oxygen isotopes of planktonic foraminifera (Huber et al. 1995). Contrary to these data, however, are recalculated paleotemperatures from foraminifers (Sellwood et al. 1994) and belemnites (Pirrie et al. 1995) which suggest that Cretaceous ocean surface temperatures were cooler.

Warm climates prevailed through the Cretaceous, and major polar glaciations were probably absent (Frakes and Frances 1988), although Weissert and Lini (1991) have suggested that small ice caps may have been present during the mid-Cretaceous. Global surface temperatures are estimated to have been at least 6°C higher than at present (Barron et al. 1995), perhaps because atmospheric p_{CO2} exceeded present-day values by two to ten times (Cerling 1991; Freeman and Hayes 1992; Berner 1994). Furthermore, the symmetrical arrangement of large landmasses around the equatorial Tethys ocean favored strong monsoonal seasonality (Parrish 1993; Jacobs and Sahagian 1995).

FACIES ASSOCIATIONS AND STRATIGRAPHIC CYCLICITY

Three unique facies associations comprise the Cupido and Coahuila platforms and represent deposition in distinct environmental settings: restricted ramp interior, peritidal shelf lagoon, and open deep platform. Interbedded evaporites and carbonates characterize a restricted lagoon located in the interior of the Coahuila ramp (Fig. 4B). Shallow subtidal and peritidal lithofacies characterize the broad shelf lagoon of the Cupido platform (Fig. 4A). Shelf-lagoon facies are interpreted to have formed in the lee of a shelf margin that changed character from a discontinuous coral–rudist reef flanking the east margin near Monterrey to a high-energy grainstone shoal fronting the south margin near Parras. The deeper, lower-energy parts of both platforms are characterized by hemipelagic mudstones and wackestones exhibiting numerous hardgrounds and firmgrounds.

Lithofacies constituting the three facies associations are typically arranged into upward-shallowing ''meter-scale cycles''. In turn, evaporitic and peritidal cycles systematically stack into ''high-frequency sequences'', which in turn are the building blocks of large-scale ''composite sequences''. This terminology is adapted from Mitchum and Van Wagoner (1991) and is used for the sequence stratigraphic framework of the Cupido and Coahuila platforms developed by Lehmann (1997). Meter-scale cycles,

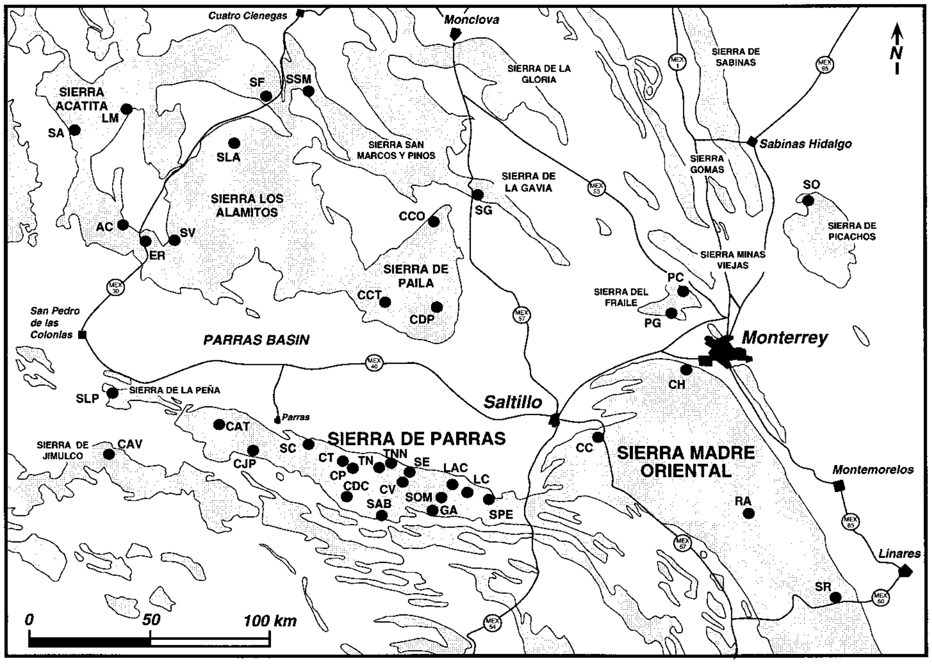

FIG. 2.—Location map of measured sections and mountain ranges with Lower Cretaceous exposures. Sections are indicated by filled circles. Ranges constituting the Coahuila block include the Sierra Acatita, Sierra Los Alamitos, and Sierra de Paila. AC = Agua Chica, CAT = Cañon Taraises, CAV = Cañon Viobora, CC = Cañon del Chorro, CCO = Casa Colorado, CCT = Cañon Corazon del Toro, CDC = Cañon de Cobra, CDP = Cañon de los Perdidos, CH = Cañon de Huasteca, CJP = Cañon de Juan Pérez, CP = Cerro Prieto, CT = Cerro de Tunal, CV = Chile Verde, ER = El Rayo, GA = Garambullo, LAC = La Casita, LC = La Concordia, LM = Las Margaritas, PC = Potrero Chico, PG = Potrero García, RA = Rayones, SA = west side Sierra Acatita, SAB = Sabanilla, SC = west side Sierra Cabrera, SE = Sierra Escondida, SF = Sierra La Fragua, SG = Sierra de La Gavia, SLA = north side Sierra Los Alamitos, SLP = Sierra de la Peña, SO = Sombreretillo, SOM = Sombrero, SPE = Sierra de Parras, east side, SSM = Sierra San Marcos y Pinos, SR = Cañon de Santa Rosa, SV = Sierra Venado, TN = Tanque Nuevo, TNN = Tanque Nuevo, north.

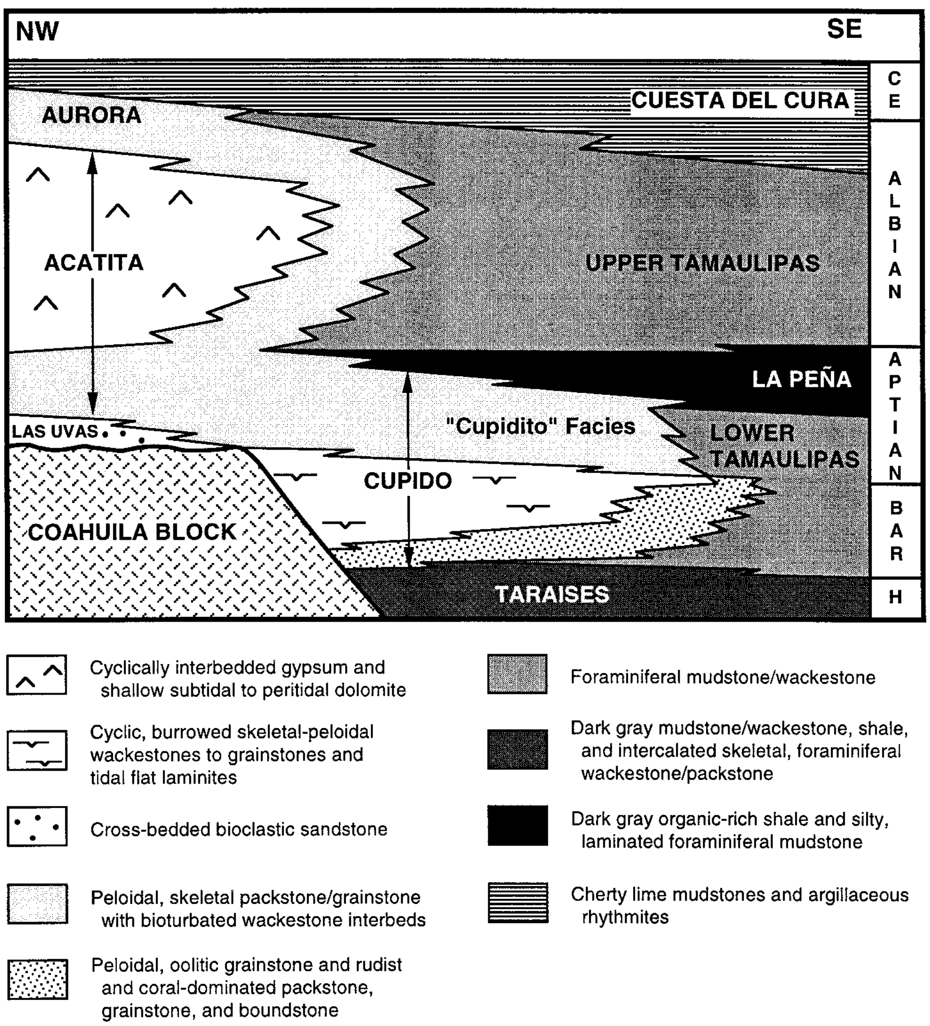

FIG. 3.—Chronostratigraphic interpretation for Barremian to Albian strata of this study (from Lehmann 1997). Chart illustrates temporal relationships between the Coahuila block to the northwest and the Sierra de Parras to the south–southeast. Note that the Las Uvas Formation and the overlying carbonates of the lower Acatita Formation are coeval with the upper transgressive part of the Cupido Formation (''Cupidito'' facies).

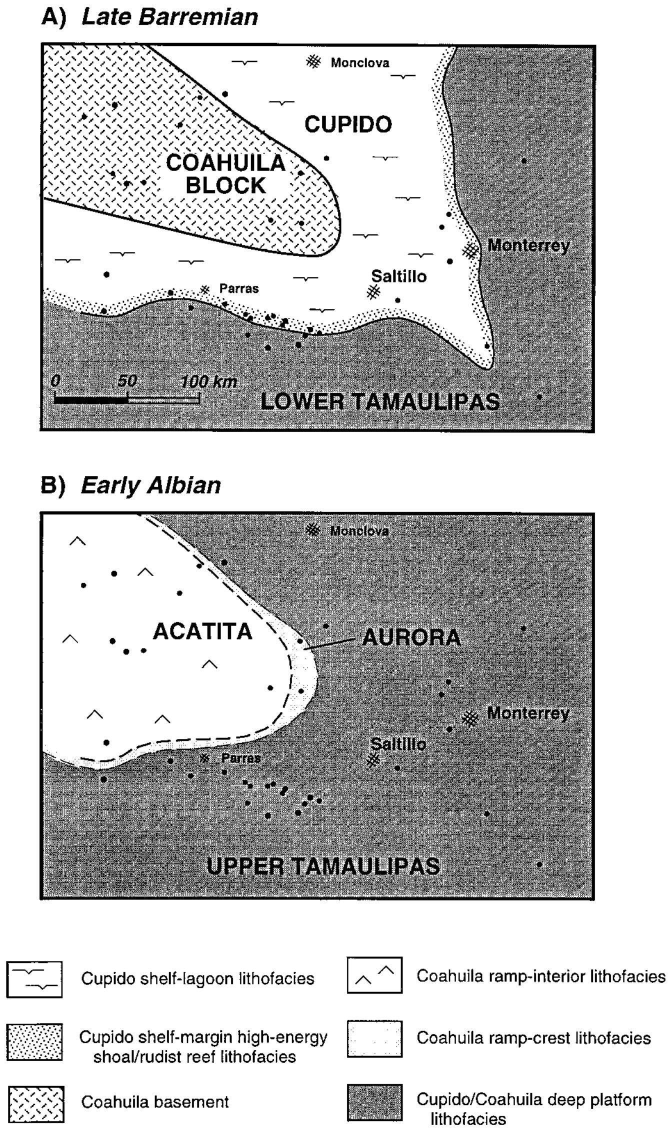

FIG. 4.—Paleogeographic maps for selected time slices across the Cupido platform (late Barremian) and Coahuila platform (early Albian) in the study area (not palinspastically corrected). Dots represent section locations. Telescoping of facies in the Sierra de Parras is related to a 30–50% shortening during the Laramide Orogeny (R. Marrett, personal communication 1995).

high-frequency sequences, composite sequences, and their disconformable bounding surfaces are interpreted to be unique chronostratigraphic entities that developed through individual cycles of accommodation change. The internal architecture of each of these genetic units consists of facies associations that are interpreted to have migrated across the platform in a predictable retrogradational, to aggradational, to progradational pattern, with the exact proportions determined by the form and magnitude of accommodation events. In the following sections, the arrangement of lithofacies into meter-scale cycles, interpretations of depositional environments, and larger-scale cycle stacking patterns are discussed for each of the three paleoenvironmental settings on the Cupido and Coahuila platforms.

Coahuila Evaporitic Ramp Interior

Carbonate and evaporite lithofacies of the Coahuila ramp interior (Acatita Formation; Table 1) are exposed in the Sierra de Paila, Sierra Los Alamitos, Sierra Acatita, and Sierra de la Peña (Figs. 2, 4B). Different thicknesses of the evaporites throughout the region (200–500 m, with the greatest thickness centered around the Sierra Acatita) suggest variable degrees of restriction of a metahaline lagoon bounded to seaward by a high-energy ramp-crest barrier. The ramp crest is exposed in only two sections composed dominantly of cross-bedded, shallow-subtidal grainstones without evaporites (Casa Colorado, Cañon de los Perdidos). The facies in these two sections are interpreted to be a high-energy shoal that isolated the Coahuila ramp interior from open-marine conditions, permitting the accumulation of thick successions of evaporitic facies. Indirect evidence for a high-energy ramp-crest shoal is the presence of skeletal packstones/grainstones both beneath and above Acatita evaporitic facies on the Coahuila block, suggesting that similar high-energy carbonates may have constituted the barrier margin contemporaneously with evaporite deposition (Fig. 3). The rest of the ramp-crest barrier is likely buried beneath Upper Cretaceous strata of the Parras foreland basin.

Lithofacies within the interior of the Coahuila platform are repetitively arranged into meter-scale cycles. Cycle thickness varies from 1 to 20 m and averages 7.8 m (total of 220 measured cycles). Within individual cycles, evaporitic facies grade upward into purely carbonate facies (Table 1; Figs. 5A, 6B–D). Evaporitic facies within any one cycle consist of $\sim$ 80% gypsiferous dolomudstones and $\sim$ 20% massive gypsum (confirmed by X-ray diffraction). Overlying carbonate facies consist of bioturbated wackestone and/or peloidal, miliolid, orbitolinid packstone/grainstone. The packstone/grainstone exhibits low-angle cross-bedding and commonly is overlain by mechanically deposited dololaminites and/or cryptalgal dololaminites (Fig. 6E). The contact between carbonate facies and overlying evaporitic facies is typically sharp, whereas transitions from evaporitic facies into carbonates are gradational. The asymmetric arrangement of lithofacies in evaporitic cycles and the nature of facies transitions are both key criteria for defining meter-scale cyclicity on the Coahuila inner ramp.

Interpretation.—Evaporites deposited in shallow-marine settings are commonly interpreted to have precipitated either on sabkha mudflats (e.g., Wilson 1967; Ruzyla and Friedman 1985; Handford 1991) or subaqueously in shallow lagoons (e.g., Davis and Nassichuk 1975; Sarg 1981; Hovorka 1987; Elliot and Warren 1989; Warren 1989). Our observations suggest that the Coahuila ramp-interior evaporites formed subaqueously because the massive gypsum beds of the ramp-interior cycles do not show features characteristic of sabkha environments. Diagnostic criteria of sabkha evaporites, such as interbedded mudcracked, cyanobacterial mats with displacive gypsum crystals or chicken-wire anhydrite after gypsum-crystal mush (Shinn 1983; Warren and Kendall 1985; Kendall 1992), are absent. Other evidence for a sabkha origin for the ramp-interior evaporites, such as erosional surfaces overlain by storm-derived detrital carbonates or eolian siliciclastics, is also not apparent. In addition, the arrangement of lithofacies within ramp-interior settings grades upward from subtidal evaporites into high-energy grainstones deposited in a beach/offshore bar setting or into low-energy tidal-flat laminites of a sabkha setting. These upper carbonate facies are disconformably overlain by the basal evaporitic facies of the succeeding cycle. Thus we interpret the massive gypsum beds to have precipitated subaqueously in the central part of a shallow lagoon, on the basis of the lack of subaerial exposure features in evaporitic lithofacies and the gradational transition into overlying shoal or tidal-flat carbonates.

Saltern deposits of widespread extent, such as the Coahuila ramp-interior evaporites, exist only in ancient platforms and have no modern analog (Warren 1989). Holocene examples of regionally limited saltern deposits are the sea-margin salinas of western Australia, Baja California, the Mediterranean, and the Middle East (Warren 1989, 1991). With the exception of Lake MacLeod of western Australia (Logan 1987), these modern saltern environments are only a few kilometers wide.

Cycle Stacking Patterns.—Individual cycles are difficult to trace laterally in Coahuila ramp-interior settings, but cycle stacking patterns reveal larger-scale, high-frequency sequences (HFSs) that can be correlated be-

TABLE 1.—*Description and interpreted depositional environments of Coahuila ramp interior lithofacies*

Lithofacies	Stratigraphic Association	Component Grains and Fossils	Sedimentary and Diagenetic Features	Interpreted Depositional Environment
mm- to cm-scale laminites	Up to 20 m thick; medium-bedded to massive; overlies peloidal, orbitolinid grainstone	whitish dolomitic silt and mud	Cryptalgal laminites; very porous; cm-to mm-scale lamination; moldic porosity after dissolution of metastable evaporites and carbonates; dissolution of gypsum pseudomorphs often obscures lamination	Upper intertidal; low-energy
cm-scale laminites	Up to 5 m thick; commonly form top of ramp interior cycles	Peloids, dolomitic silt and mud	Horizontal mechanical lamination; low-angle cross-lamination; very porous; moldic porosity after dissolution of metastable evaporites and carbonates	Intertidal to shallow subtidal; moderate-energy
Peloidal, orbitolinid, grainstone	Up to 30 m thick; form top of cycles or are overlain by cm-scale laminites and/or mm- to cm-scale laminites	Shell fragments, peloids orbitolinids, miliolids, rudists, mainly requienids, caprinids and *Toucasia*	Low-angle cross lamination; horizontal lamination	Shallow subtidal shoal; high-energy
Bioturbated wackestone	Up to 2 m thick; intermediate facies, rarely form top of ramp interior cycles	Peloids, benthonic foraminifers, requienids and *Toucasia*	Coarse saddle dolomite obscures original composition; homogeneous or extensively bioturbated	Shallow-subtidal lagoon; low/moderate energy
Massive gypsum	Up to 8 m thick; <1 m beds more common; interlayered with homogeneous lime mudstone or dolomite with gypsum; may form base of ramp-interior cycles	cm-thick gypsum layers alternating with mm-thick gray carbonate-mud layers	Lamination of mm-thick mud and evaporite layers; commonly recrystallized; chaotic fabric	Restricted, hypersaline, subtidal lagoon; low-energy
Homogeneous mudstone with gypsum	Up to 15 m thick; form base of ramp-interior cycles; commonly massive	Fine- to medium-crystalline dolomite and gypsum	Poorly indurated, homogeneous, partially bioturbated	Restricted, hypersaline to normal marine subtidal lagoon; low-energy

tween isolated sections (Fig. 5B; Lehmann 1997). Similarly to the arrangement of lithofacies in meter-scale evaporitic cycles, HFSs shallow upward from generally thicker-than-average evaporite-dominated cycles to generally thinner-than-average carbonate-dominated cycles (Fig. 6A). The cycle number and thickness of cycles in individual HFSs can be highly variable from section to section even though the overall upward-shallowing pattern is evident. In the example in Figure 5B, HFS3 contains 8 cycles and is 86 m thick at Sierra Acatita, whereas at Cañon Corazon del Toro only five cycles are recognized and the thickness decreases to 44 m. These lateral changes in the thickness, lithofacies, and number of ramp-interior cycles in HFSs suggest that the Acatita evaporitic lagoon had some subtle bathymetric relief and might have been divided into sub-basins. Even along single depositional surfaces, the distribution of subenvironments was probably a mosaic of brine pans and mudflats, a pattern common in modern shallow evaporitic lagoons (Warren 1989; Warren and Kendall 1985; Kendall 1992). Such depositional variability along individual time lines would have contributed to the internal variability of single HFSs across the Coahuila ramp.

In the example (Fig. 5B), four HFSs constitute a single composite sequence. The ratio of carbonate-dominated cycles to evaporite-dominated cycles within HFS1 through HFS4 increases toward the top of the composite sequence. Uppermost HFS4 is on average the thinnest in the HFS stack and is dominated by tidal-flat facies, reflecting progradation of peritidal carbonate environments over the evaporitic lagoon in response to minimal long-term accommodation. The composite sequence boundary is placed at the top of tidal-flat-dominated cycles in HFS4 on the basis of the relatively abrupt transition into thick evaporite cycles of the overlying composite sequence.

Cupido Peritidal Shelf Lagoon

The broad Cupido shelf lagoon is bounded along its seaward edge by a shelf margin that varies in character along strike (Fig. 4). From the Sierra de Jimulco through the northern part of the Sierra de Parras and continuing eastward into the main Sierra Madre Oriental near Saltillo (Figs. 1, 4A), the shelf margin is composed of a fringe of high-energy grainstone shoal deposits. The margin makes a sharp dogleg northward where it changes to rudist and coralline reefal facies along the gulfward side of the platform (Wilson 1975; Conklin and Moore 1977; Wilson and Pialli 1977; Wilson et al. 1984; Goldhammer et al. 1991).

The grainstone shoal margin in the northern Sierra de Parras is predominantly composed of peloids and ooids but exhibits subordinate layers (1–5 m thick) of caprinid and requienid rudists (Table 2). Shoal architecture consists of large-scale, progradational, sigmoidal clinoforms dipping up to 25° to the south–southwest. The contiguous shoal margin and reef margin of the Cupido platform formed a physical barrier separating a peritidal shelf lagoon to the north and west from a deep-water, low-energy shelf to the south and east (Lower Tamaulipas Formation).

Cupido shelf-margin shoal and reefal facies are overlain by variable thicknesses of peritidal lithofacies, which are interpreted to have developed on the broad, low-energy shelf lagoon in the lee of the margin (Fig. 4A). The thickness of peritidal lithofacies ranges from 400 to 660 m along the north side of the Sierra de Parras. Peritidal lithofacies form cyclic arrangements similar to those recognized throughout the stratigraphic record (Pratt et al. 1992). The thickness of individual peritidal cycles in the Cupido Formation in the Sierra de Parras ranges from 0.5 to 28.5 m with an average of 4.9 m (total of 686 measured cycles). More than 90% of the peritidal cycles are thinner than 10 m.

Lithofacies transitions within Cupido peritidal cycles are gradational and progressively fine upward (Table 2; Figs. 7, 8). Contacts between adjacent cycles are typically sharp. A thick-bedded to massive peloidal grainstone forms the basal lithofacies of a typical Cupido peritidal cycle and commonly contains whole to fragmental caprinid and requienid rudists. Bioturbation and lime mud content increase upward in the basal unit, and the carbonates become lighter gray because of increasing amounts of dolomite. Intermediate facies are commonly wackestones containing requienid rudists and *Chondrodonta* bivalves; these wackestones fine upward to a structureless/fenestral dolomudstone. Calcite pseudomorphs after gypsum may be present in the mudstones. Commonly, cryptalgal laminites overlie structureless/fenestral mudstones, capping the cycle. The laminites are mudcracked, contain rip-up clasts, and rarely exceed 0.5 m in thickness (Fig. 8F). The mudstone or laminite caps are sharply overlain by basal grainstone of the overlying cycle.

Interpretation.—Evidence for upward shallowing within a Cupido peritidal cycle is provided by (1) upward decrease in shallow-subtidal components, such as ooids, shell fragments and intraclasts; (2) upward transition from a normal marine faunal association with caprinids, miliolids, and green algae to a more restricted requienid–*Chondrodonta* faunal association; and (3) capping lithofacies that exhibit calcite pseudomorphs after gypsum, mudcracks, and rip-up clasts, indicating semiarid conditions and episodic subaerial exposure. The sharp contact between the top of a peri-

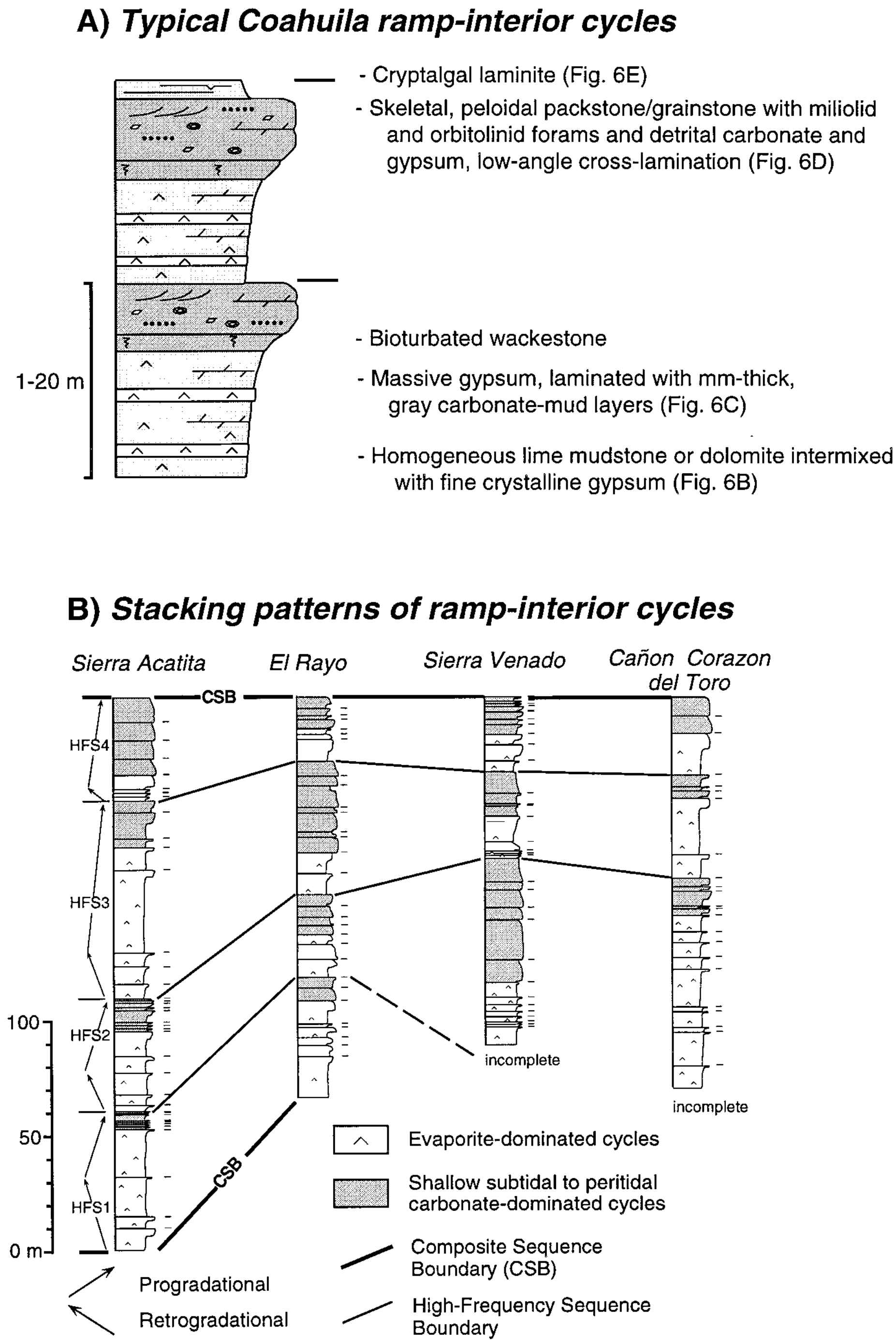

FIG. 5.—**A)** Typical Coahuila ramp-interior evaporitic cycles. **B)** Stacking patterns of ramp-interior cycles into high-frequency sequences within a single composite sequence. See Figure 2 for section locations. In general, high-frequency sequences on the Coahuila block shallow upward from evaporite-dominated cycles to carbonate-dominated cycles. Tick marks to right of each section mark cycle boundaries.

tidal cycle and the base of the overlying cycle suggests abrupt flooding. Similar arrangements of peritidal cycle lithofacies on Cretaceous carbonate platforms have been observed on the Cupido shelf near Monterrey (Goldhammer et al. 1991), in the El Abra Formation of the Valles platform of east-central Mexico (Minero 1988, 1991), on the Gavrovo platform of northwestern Greece (Grötsch 1996), and on Pacific guyots (Röhl and Ogg 1996).

Cycle Stacking Patterns.—Peritidal cycles of the Cupido shelf lagoon stack into intermediate-scale high-frequency sequences (HFSs) that can be correlated between isolated sections in the Sierra de Parras (Fig. 7B; Lehmann 1997). The number of cycles within HFSs is variable, but each HFS is distinguished by vertical stacking patterns of generally thicker-than-average, subtidal-dominated cycles low in each HFS, to generally thinner-than-average, tidal-flat-dominated cycles high in each HFS. In the example in Figure 7B, four HFSs stack into one composite sequence. The lowermost HFS in this composite sequence is the thickest of the four (50–130 m), contains the greatest number of meter-scale cycles of all four HFSs, and exhibits a high percentage of subtidal facies. Overlying HFSs within the composite sequence thin upward with the youngest HFS being the thinnest (20–45 m), containing the least number of cycles, and exhibiting the highest proportion of tidal-flat facies. The upper composite sequence boundary is defined at the top by thin peritidal cycles that are immediately overlain by thick subtidal facies of the base of the overlying composite sequence.

These HFS stacking patterns are interpreted to reflect a long-term com-

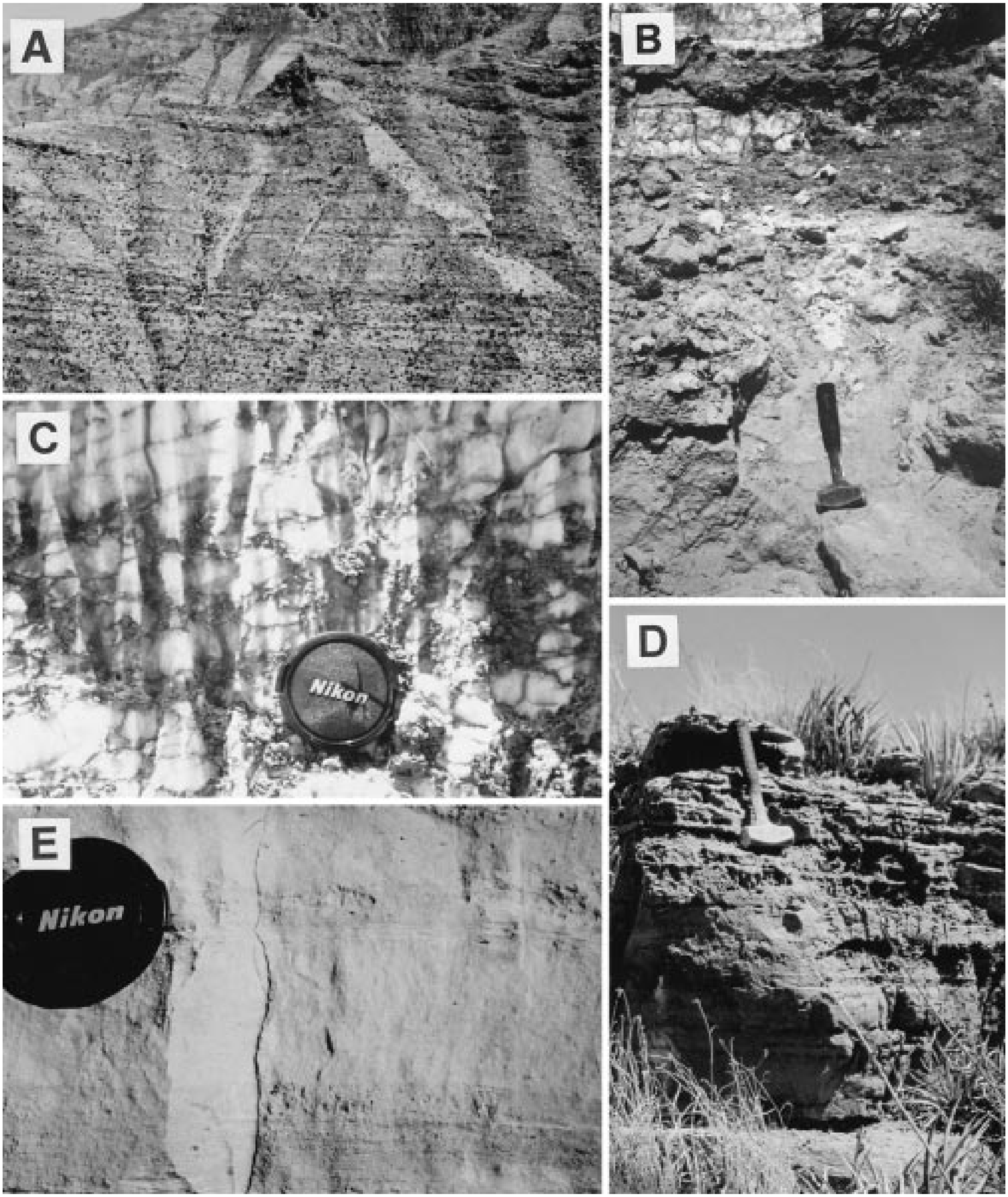

FIG. 6.—**A)** Outcrop of ramp-interior cycles, west side of Sierra Acatita. Lighter-weathering units are thicker-than-average evaporite-dominated cycles, and darker-weathering units are thinner-than-average carbonate-dominated cycles. **B)** Basal lithofacies of ramp-interior cycles: homogeneous, gypsiferous mudstone with intercalated massive gypsum beds. **C)** Detailed view of massive gypsum interbed within basal lithofacies of cycles. **D)** Low-angle cross-laminated, peloidal, orbitolinid grainstone forms middle to upper parts of typical ramp-interior cycles. **E)** White, millimeter- to centimeter-scale, laminated dolomudstone with moldic porosity commonly forms cap of ramp-interior cycles.

TABLE 2.—*Description and interpreted depositional environments of Cupido peritidal shelf-lagoon and shelf-margin lithofacies*

Lithofacies	Stratigraphic Association	Component Grains and Fossils	Sedimentary and Diagenetic Features	Interpreted Depositional Environment
mm- to cm-scale laminites	Up to 0.5 m thick; commonly overlies structureless/fenestral mudstone	Dolomitic silt and mud; cm-thick peloidal grainstone layers intercalated	Cryptalgal laminites; mudcracks; rip-ups; fenestrae; calcite pseudomorphs likely after gypsum; dolomitization	Upper to lower intertidal; protected peritidal zone
Structureless/fenestral mudstone	Up to 8 m thick; thin- to medium-bedded; overlies bioturbated, requienid wackestone	Dolomitic silt and mud, requienids, *Chondrodonta* bivalves	Rare bioturbation; fenestrae; calcite pseudomorphs likely after gypsum; dolomitization	Intertidal to shallow subtidal; protected peritidal zone
Bioturbated, requienid wackestone	Up to 15 m thick; massive to thick-bedded; cliff-former; overlies peloidal, skeletal grainstone	Peloids, intraclasts, benthonic foraminifers, miliolids, rudists (mainly requienids), *Chondrodonta* bivalves, shell fragments, gastropod *Nerinea*	Bioturbation; mottled or homogeneous appearance; less common low-angle cross-lamination; burrows preferentially dolomitized	Shallow subtidal; above fair-weather wave base
Peloidal, skeletal packstone and grainstone	Up to 20 m thick; massive to thick-bedded; cliff-former; overlies peloidal-skeletal grainstone lithofacies	Peloids, ooids, oncoliths, green algae, echinoids, shell-fragments, gastropod *Nerinea,* benthonic foraminifers, miliolids, rudists (caprinids and requienids), intraclasts	Cross-bedding; low-angle cross-lamination; bioturbation; common partial dolomitization; less common complete dolomitization	Shallow subtidal; above fair-weather wave base
Peloidal, skeletal, oolitic grainstone	Thickness ranging from 60 m to 400 m at shelf-margin; massive; extensive cliff-former; overlies mudstone/wackestone and shales and is overlain by peritidal lithofacies	Peloids, benthonic foraminifers, ooids; thickets of rudists up to 5 m thick composed of requienids and caprinids	Large-scale sigmoidal clinoforms downlapping onto underlying mudstones/wackestones and shales; cross-bedding; extensive dolomitization	Subtidal shelf-margin shoal; high-energy; above fair-weather wave base

posite cycle of accommodation change. The lowermost HFS exhibits characteristics of increasing accommodation and is interpreted to reflect retrogradational to aggradational accumulation on the Cupido shelf. Overlying thinner HFSs are explained by progressively decreasing accommodation and dominantly progradational migration of peritidal facies tracts. The lateral thickness differences within individual HFSs in the composite sequence may be attributable to variations in subsidence rates, sediment production rates, or sediment distribution patterns. Systematic changes in relative cycle thickness and composition at the HFS scale are consistent within each section, however, regardless of total thickness differences between sections.

Cupido and Coahuila Open-Marine Deep Platform

Deep platform lithofacies (Lower/Upper Tamaulipas Formation) are located in the southern part of the Sierra de Parras, the eastern Sierra Madre Oriental between Monterrey and Linares, and in mountain ranges and potreros east of the Sierra de Paila (Table 3; Figs. 2, 4). Foraminiferal wackestones and lime mudstones make up the majority of the rock types in this facies association and typically form monotonous thin- to thick-bedded successions (Figs. 9, 10A). The majority of the allochems in the wackestones and lime mudstones are planktonic foraminifers, ostracodes, calcispheres, and nannoconids, with a subordinate component of echinoderm and rudist fragments.

Regularly spaced firmgrounds and less common hardgrounds interrupt the succession and have been observed at several deep ramp sections in the Upper Tamaulipas Formation (Fig. 9B). Hardgrounds are synsedimentary, lithified seafloors, which indicate prolonged phases of nondeposition or slow sedimentation rates (Purser 1969; Bathurst 1971; Bromley 1975; Fürsich 1979). Firmgrounds develop at the early stages of hardground formation and form after an initial bioturbation phase followed by prolonged omission, during which initial compaction, erosion, and a varying degree of cementation take place.

On the Coahuila deep ramp, firmgrounds form irregular surfaces with up to 20 cm relief within monotonous foraminiferal wackestone and lime mudstone facies (Fig. 10B). They are distinguished by a consistent, 30-cm-thick diffuse zone of finely crystalline dolomite directly above the firmground containing subangular to subrounded intraclasts of the underlying nondolomitized foraminiferal wackestone. In contrast, hardgrounds do not show pronounced relief, but rather form a sharp surface that is commonly overprinted by pressure-solution features, such as stylolites and wispy seams containing residues of clay minerals and organic matter (Fig. 10C). A 5-cm-thick, diffuse zone of finely crystalline dolomite directly above the hardground contains nondolomitized, small shell fragments and subangular to subrounded intraclasts composed of nondolomitized foraminiferal wackestone.

Firmgrounds and hardgrounds, representing episodes of nondeposition or slow sedimentation, separate individual depositional units of mudstone/wackestone lithofacies. Thus, in a genetic sense, the disposition of firmgrounds and hardgrounds within an otherwise monotonous succession of hemipelagic foraminiferal wackestones and lime mudstones can be regarded as a ''cyclic'' arrangement, manifesting the alternation of depositional and nondepositional events. The number of firmgrounds and hardgrounds intercalated in deep ramp sections of the Upper Tamaulipas Formation ranges from 40 at Huasteca Cañon (190 m of total section) to 26 at Cañon del Chorro (150 m of total section). Correlation of individual firmgrounds and hardgrounds between sections is not reliable, and even broader-scale vertical distribution patterns are difficult to correlate with confidence (Fig. 9B).

Interpretation.—Deposition in the deeper waters surrounding the Cupido and Coahuila shallow-water platforms was dominantly hemipelagic, with the majority of the mud originally generated on the platform top. The planktonic foraminifers, ostracodes, calcispheres, and nannoconids were deposited as a pelagic rain by suspension settling. The minor amounts of echinoderm and rudist debris indicate occasional sediment transport of larger grains from the platform margin. Because of the lack of storm beds or storm-reworked clasts, we interpret the wackestones and lime mudstones to have been deposited below storm-weather wave base (Aigner 1985), perhaps in waters deeper than ~ 100 m. However, storms might have swept carbonate clasts from the platform margin onto the deep platform. It is important to note that the muddy sediment of the Cupido and Coahuila deep platforms was significantly shallower than true basinal muds that accumulated in kilometer-deep waters of the ancestral Gulf of Mexico.

CONTROLS ON CYCLE DEVELOPMENT

A compilation of published interpretations for Cretaceous meter-scale cycles deposited in subenvironments across shallow carbonate platforms shows eustasy to be the prevailing interpretation as the dominant causal mechanism (Table 4). Data from the Cupido and Coahuila platforms support a similar conclusion, and in a subsequent section we propose a depositional model that illustrates how the same eustatic signal may affect cycle generation in each of the three paleoenvironmental settings. Other processes, however, such as climate change and autogenic shifts in deposition, may have exerted a significant, but likely subordinate, influence on cycle development. Global climate change ultimately controls eustasy, e.g.,

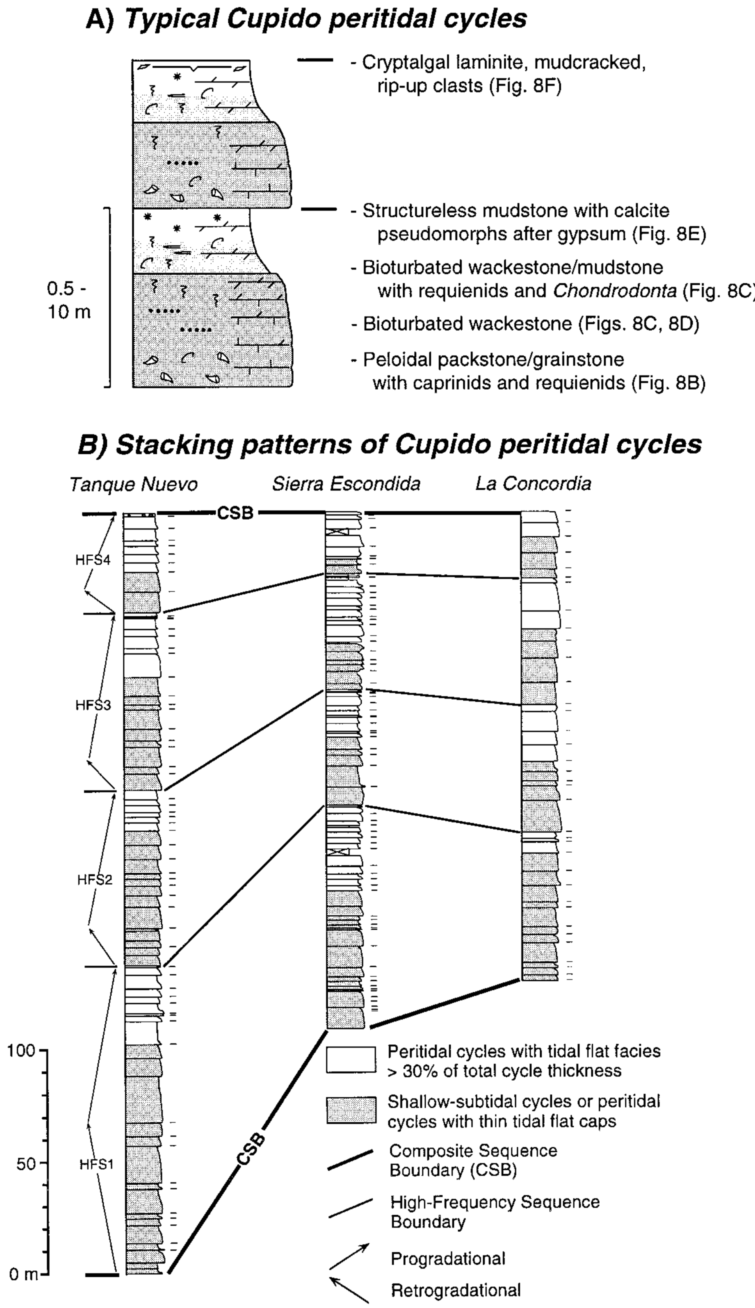

FIG. 7.—**A)** Typical Cupido peritidal cycles. **B)** Stacking patterns of peritidal cycles into high-frequency sequences within a single composite sequence in the Cupido Formation. See Figure 2 for section locations. In general, high-frequency sequences on the Cupido shelf grade upward from shallow subtidal-dominated cycles to peritidal-dominated cycles. Tick marks to right of each section mark cycle boundaries.

by thermal contraction and expansion of sea water and/or melting of glaciers and polar ice caps. However, it is not clear how global climate affects sea level during peak greenhouse times. In addition, regional climatic effects might influence depositional environments independently of these global climatic changes. Therefore, in the following sections climate is discussed separately from eustasy as a controlling factor on cycle development specifically for the Cupido and Coahuila platforms. Furthermore, the scale-independent architectural similarities between meter-scale cycles, high-frequency sequences, and composite sequences on both platforms are used to infer that these causal mechanisms must have been influential over a range of timescales.

Coahuila Ramp-Interior Evaporitic Cycles

Interbedded carbonates and evaporites are commonly cyclically arranged, but the precise mechanisms governing cycle development are difficult to isolate (Kendall 1988, 1992). Any depositional model for evaporitic cycles must incorporate a few fundamental requirements of evaporite formation. Brine concentration and composition are the basic controls on evaporite precipitation and are ultimately influenced by the inflow/outflow ratio to a lagoon or basin (Logan 1987; Kendall 1988). In turn, the hydrology of the lagoon, climate, and relative sea-level fluctuations are critical factors that affect the inflow/outflow ratio. Hydrologic conditions in the restricted interior of the Coahuila ramp were likely governed by exchange across a ramp-crest barrier shoal that separated the open ocean from the lagoonal inner ramp. The two most viable mechanisms contributing to changes in the inflow/outflow ratio across the barrier shoal and the consequent development of Coahuila ramp-interior cycles are climate and eustasy, acting either independently or perhaps in concert with one another. If climate or eustasy acted independently, then each control must be able to explain the upward shallowing and asymmetric arrangement of lithofacies within evaporitic cycles.

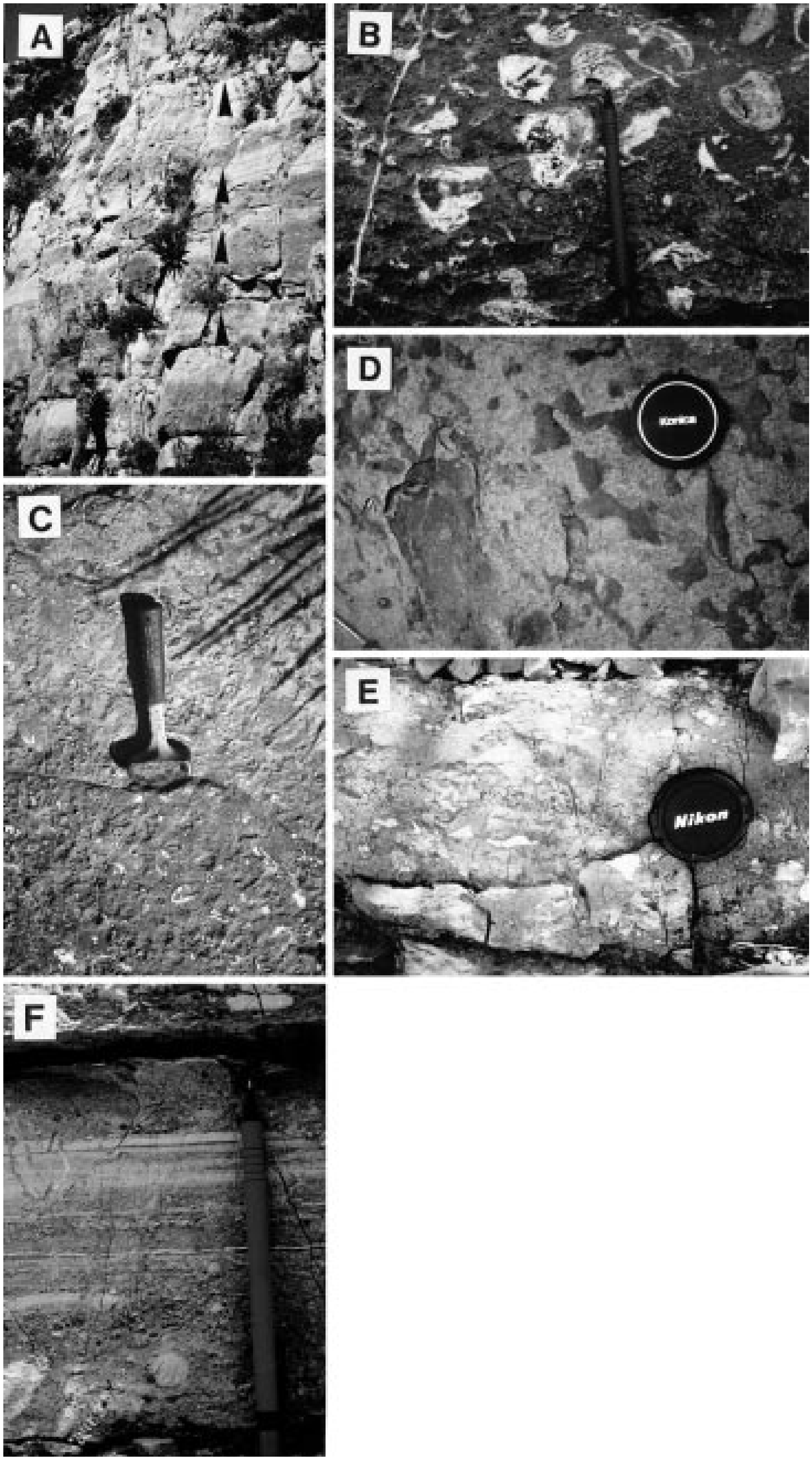
A
B
C
D
E
F
Nikon

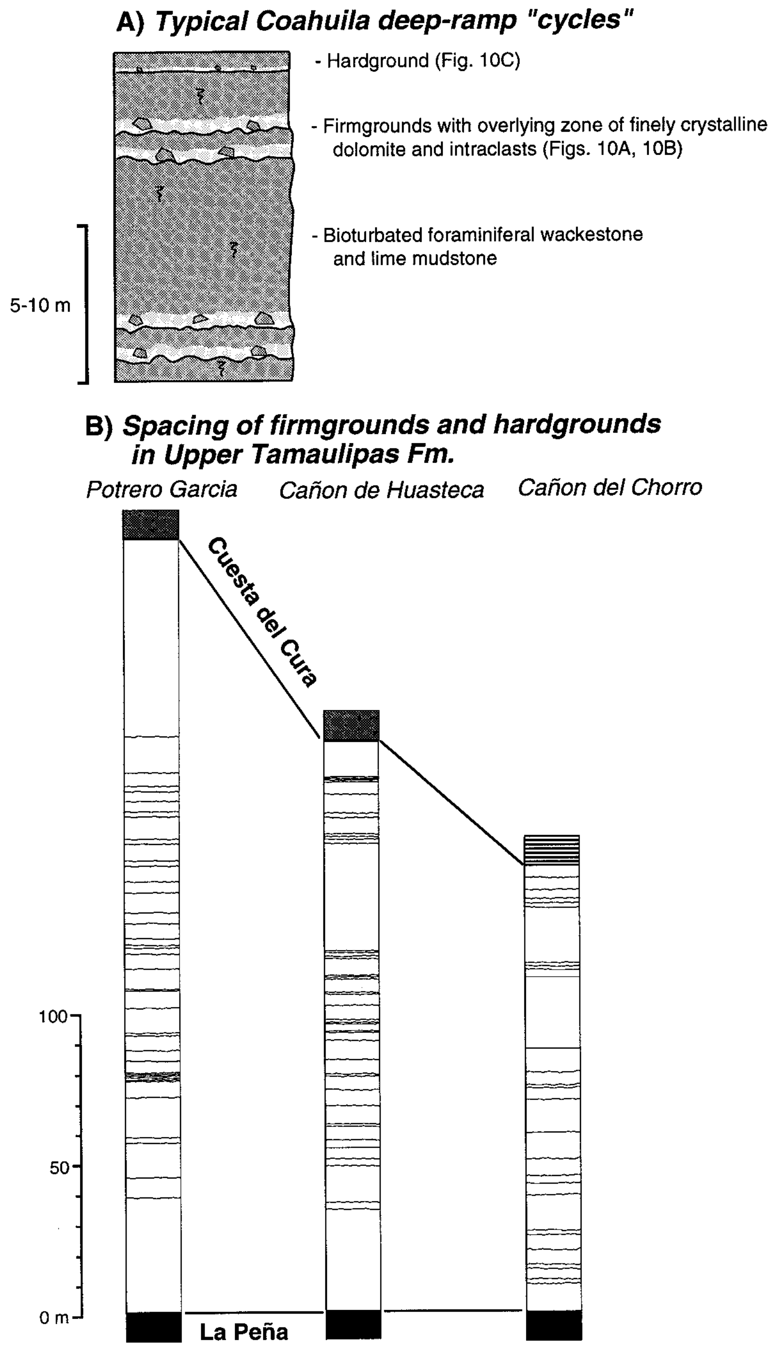

FIG. 9.—**A)** Typical deep-ramp ''cycles'' of the Upper Tamaulipas Formation. **B)** Three complete sections from the Upper Tamaulipas Formation. White background is monotonous lime mudstone and foraminiferal wackestone. Firmgrounds are shown as wavy lines and hardgrounds are shown as straight lines. The majority of syndepositional diagenetic surfaces in the Upper Tamaulipas are firmgrounds.

Climate.—Evaporites form in arid to semiarid regions where the potential exists that more water leaves a basin or a lagoon by evaporation or surface/subsurface outflow than enters through rainfall or surface/subsurface inflow. The Coahuila carbonate ramp was located at approximately 28° N during the Early Cretaceous (Barron et al. 1981). This is the latitude of modern desert belts where dry, cold air descends in the Hadley cell, absorbs water, and creates ideal conditions for evaporation (Warren 1989). Changes in regional climate, operative over several timescales and perhaps expressed by the intensity and frequency of tropical storms and monsoons, affect the concentration of brines in metahaline lagoons and may initiate

←

FIG. 8.—**A)** Field photograph showing several peritidal cycles, Chile Verde. Cycle tops are marked by arrows. Note the color difference between the darker-gray shallow-subtidal facies, which are predominantly calcitic, and the lighter-gray, dolomitized intertidal deposits. **B)** Peloidal, skeletal grainstone with caprinid rudists, commonly forming the base of peritidal cycles. **C)** Gradational transition between a peloidal, skeletal grainstone containing fragments of caprinid rudists and overlying bioturbated, peloidal wackestone. Size of the rudist fragments gradually decreases upward, whereas the intensity of bioturbation increases. **D)** Bioturbated peloidal wackestone with preferentially dolomitized burrows. **E)** Structureless/fenestral mudstone with calcite pseudomorphs after gypsum. **F)** Tidal-flat laminites with rip-up clasts and mudcracks.

TABLE 3.—*Description and interpreted depositional environments of Cupido and Coahuila deep-platform lithofacies*

Lithofacies	Stratigraphic Association	Component Grains and Fossils	Sedimentary and Diagenetic Features	Interpreted Depositional Environment
Foraminiferal wackestone	Thin- to thick-bedded; interbedded with lime mudstone; dominant deep-platform lithofacies	Micro-peloids, intraclasts, planktonic foraminifers, ostracodes, calcispheres, sponges, nannoconids, ammonites, bivalves, rudist fragments, echinoids, brachiopods	Bioturbation, firmgrounds, hardgrounds, commonly homogeneous, low-angle cross lamination, graded rhythmic lamination, chert nodules	Deep subtidal; oxygenated; below storm-weather wave base
Lime mudstone	Thin- to thick-bedded; interbedded with foraminiferal wackestone; some 20 cm-thick shale layers intercalated	Planktonic foraminifers, ostracodes, calcispheres, sponges, nannoconids, ammonites	Bioturbation, chert nodules	Deep subtidal; oxygenated; below storm-weather wave base

cyclic shifts from precipitation of evaporites to carbonate deposition (Fig. 11A). In the Coahuila ramp interior, the basal mudstone/gypsum lithofacies of the evaporitic cycles likely formed during arid phases, which promoted concentration of brines and subaqueous precipitation of evaporites. As climate changed toward increased seasonal rainfall and higher humidity, the inflow/outflow ratio increased, slowing evaporation and causing brines to become more dilute. Migration of adjacent carbonate environments over the formerly evaporitic lagoon may have occurred in response to a shift to more normal-marine water composition (independently of any change in base level). Shoalwater packstone/grainstones and peritidal laminites de-

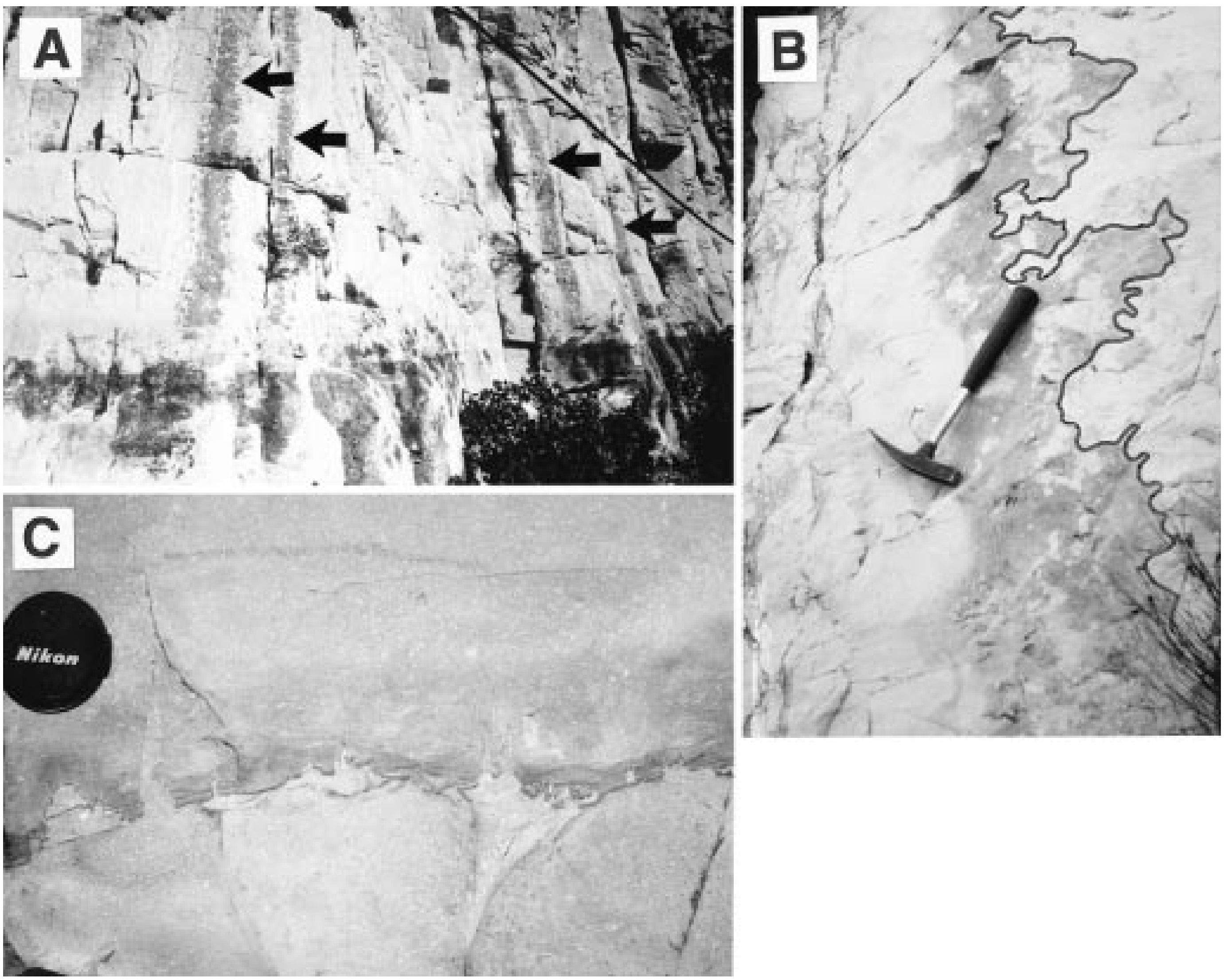

FIG. 10.—**A)** Field photo of deep-ramp facies, Upper Tamaulipas Formation, Cañon de Huasteca. Beds are vertical and stratigraphic ''up'' is to the left. The firmgrounds (shown by arrows) frequently form pairs separated by several meters of monotonous foraminiferal wackestone. The darker bands are dolomitized intervals above the firmgrounds. The distance between the two firmgrounds on the left is about 1 m. Field photo shows two pairs. **B)** Cañon del Chorro; stratigraphic ''up'' is to the left. Firmgrounds form an irregular surface with up to 20 cm relief within monotonous foraminiferal wackestone and lime mudstone facies. Overlying this surface (indicated by thin pen line) is 30-cm-thick diffuse zone of finely crystalline dolomite containing subangular to subrounded intraclasts of the underlying nondolomitized foraminiferal wackestone. **C)** Hardground, Cañon de Huasteca, overprinted with stylolite (4–5 cm amplitude) with diffuse 5-cm-thick zone of dolomite above.

TABLE 4.—*Examples of Cretaceous evaporitic, shallow-subtidal, and peritidal cycles*

Age	Location	Platform/Basin	Depositional Setting	Cycle Type	Suggested Mechanism	Reference
Albian	Texas	Northern Gulf Coast (Ferry Lake Anhydrite)	Evaporitic lagoon	Carbonate-to-evaporite alternations	Eustasy	Loucks and Longman 1982; Warren 1989
Hauterivian-Albian	Mid-Pacific	Resolution Guyot (Pacific)	Shallow-subtidal to peritidal	Shallow-subtidal to peritidal	Eustasy	Arnaud et al. 1995
Aptian-Albian	Mid-Pacific	Pacific Guyots	Lagoon	Shallow-subtidal to peritidal	Eustasy	Röhl and Ogg 1996
Barremian-upper Albian	Greece	Gavrovo Platform	Peritidal	Peritidal	Eustasy	Grötsch 1996
Barremian-lower Aptian	Slovenia	Dinaric Platform	Shallow subtidal	Shallow-subtidal	Eustasy	Grötsch 1994
Aptian-Maastrichtian	Southeastern Yugoslavia	Adriatic and Dinaric Platform	Subtidal to supratidal backreef	Peritidal and subtidal lagoon	Not mentioned	Obradović et al. 1993
Middle Cenomanian-lower Campanian	Italy	Maiella Platform	Platform margin to peritidal	Rudist rudstone-to-bioclastic sandstone-to-rudist biostrome, may be peritidal capped	Not mentioned	Eberli et al. 1993
Barremian	Italy	Monte Raggio	Peritidal	Peritidal	Eustasy	Longo et al. 1994
Hauterivian-Albian	Southeastern France, Swiss Jura	Urgonian Platform	Shallow-subtidal to peritidal	Shallow-subtidal to peritidal	Eustasy	Arnaud-Vanneau and Arnaud 1990; Hunt and Tucker 1993
Berriasian	Switzerland, France	Purbeckian	Peritidal	Peritidal	Climate-controlled sea-level changes	Strasser 1988
Albian-Cenomanian	Spain	Iberian Basin	Continental to shallow marine	Mixed carbonates and siliciclastics	Eustasy	García et al. 1993
Cenomanian-Turonian	Spain	Iberian Basin	Shallow ramp	Coarsening-upward shallow-subtidal and peritidal	Eustasy	Valladres et al. 1996
Late Cenomanian-early Turonian	Spain	Iberian Basin	Shallow ramp to basin	Limestone-marl, grainstone-rudist dolostone, and peritidal	Eustasy	Segura et al. 1993
Upper Coniacian-lower Campanian	Spain	Iberian and Prebetic Ranges	Shallow-subtidal to exposure	Shallow-subtidal carbonates capped by paleosols	Eustasy	Martín-Chivelet and Giménez 1992
Albian-Cenomanian	Spain	Platforms of the Iberian Ranges	Shallow-subtidal to peritidal	Mixed carbonates and siliciclastics	Eustasy	García et al. 1996
Portlandian-Berriasian	Southern Spain	Prebetic	Peritidal	Peritidal	Glacio-eustatic sea-level changes	de Cisneros and Vera 1993
Barremian-Aptian	Northeast Mexico	Cupido Platform	Peritidal	Peritidal	Eustasy	Goldhammer et al. 1991
Albian	East-central Mexico	Valles Platform	Peritidal	Peritidal	Eustasy	Minero 1988, 1991
Early Aptian-Albian	Venezuela	Maracaibo Platform	Protected lagoon to open-marine shelf	Shallow-subtidal to peritidal, mixed carbonates and siliciclastics	Not mentioned	Vahrenkamp et al. 1993

posited on top of evaporitic facies in ramp-interior cycles may record the gradual transition from hyperaridity to less arid conditions.

The now-peritidal Coahuila lagoon must have undergone a nondepositional lag time coincident with a return to more arid conditions to produce the sharp contact between tidal-flat carbonates of the cycle cap and overlying saltern evaporite facies of the succeeding cycle. During this transitional phase, the lagoon subsided continuously and the earliest evaporites to precipitate after the brines reached saturation stages might have cemented the underlying carbonates to produce a hydroseal (Elliot and Warren 1989). With progressive climate shift toward hyperaridity, massive evaporites formed in concert with dolomudstones in the shallow lagoon.

Eustasy.—High-frequency eustatic changes have been suggested as the primary mechanism behind the deposition of carbonate–evaporite cycles on other platforms (Table 4). Eustatic changes operative over several timescales may have affected the Coahuila ramp interior by changing the geometry of the ramp-crest barrier shoal separating the inner ramp from the open ocean. At the beginning of each cycle (Fig. 11B), rapid eustatic rise might have forced the aggradational growth of the ramp crest in an effort to keep up with increasing accommodation, in the process creating a shallow subtidal lagoon cut off from the open ancestral Gulf. As brines in the interior of the low-energy lagoon became more concentrated, evaporites precipitated within lime muds or as massive gypsum beds. Early evaporitic cements might have hydrosealed the lagoon substrate, further enhancing the concentration of brines by reducing subsurface meteoric inflow. Normal-marine waters may have episodically replenished the interior lagoon during this phase of increasing accommodation, providing the supply of salts that fostered precipitation of thick accumulations of evaporites.

As sea-level rise slowed, the ramp crest and marginal tidal-flat facies tracts prograded over the lagoon, depositing high-energy grainstones and tidal-flat facies on top of evaporitic lagoonal facies. As all available accommodation space eventually filled, production of carbonate sediment slowed. Local brine pans may have remained in the platform interior, on the basis of environmental mosaics common to modern evaporitic settings. After a nondepositional lag time and subsequent eustatic rise, the ramp crest aggraded in response to increased accommodation and once again formed a restricted lagoon in which subtidal evaporitic lithofacies of the overlying cycle were deposited. A similar model of ''transgressive evaporite'' and ''regressive carbonate'' was proposed by Tucker (1991) for the Upper Permian (Zechstein) of northeast England and the North Sea.

Cupido Peritidal Cycles

Climate.—Orbitally driven climate variations affecting deep-ocean sedimentation are well documented for the Cretaceous greenhouse world (de Boer 1982; Schwarzacher and Fischer 1982; Herbert and Fischer 1986), but climatic variability is difficult to recognize on shallow carbonate platforms. Mutti and Weissert (1995) were able to identify several sedimentologic and diagenetic features within individual bed sets of Triassic carbonates indicative of monsoonal climatic changes on the 10^5 year scale. Similar evidence for short-term climatic changes controlling development of peritidal cycles on the Cupido shelf lagoon is limited because of the absence of diagnostic indicators of humid climates, such as interbedded continentally derived siliciclastics, paleokarst, and paleosols.

The La Virgen evaporites deposited to the north of the study area contemporaneously with the Cupido carbonate platform indicate that an arid to semiarid climate prevailed during the time the peritidal cycles were deposited. These evaporitic facies would have been highly sensitive to climatic changes that would have altered the inflow/outflow ratio of the lagoon (as previously discussed). In contrast, purely carbonate peritidal cycles forming on the Cupido shelf lagoon would be expected to have exhibited much less sedimentologic response to long-term changes in relative rainfall. Peritidal sedimentation would instead have been more directly influenced by global or regional *surface temperature* changes that would have affected the productivity of carbonate-secreting organisms. Hardie (1986)

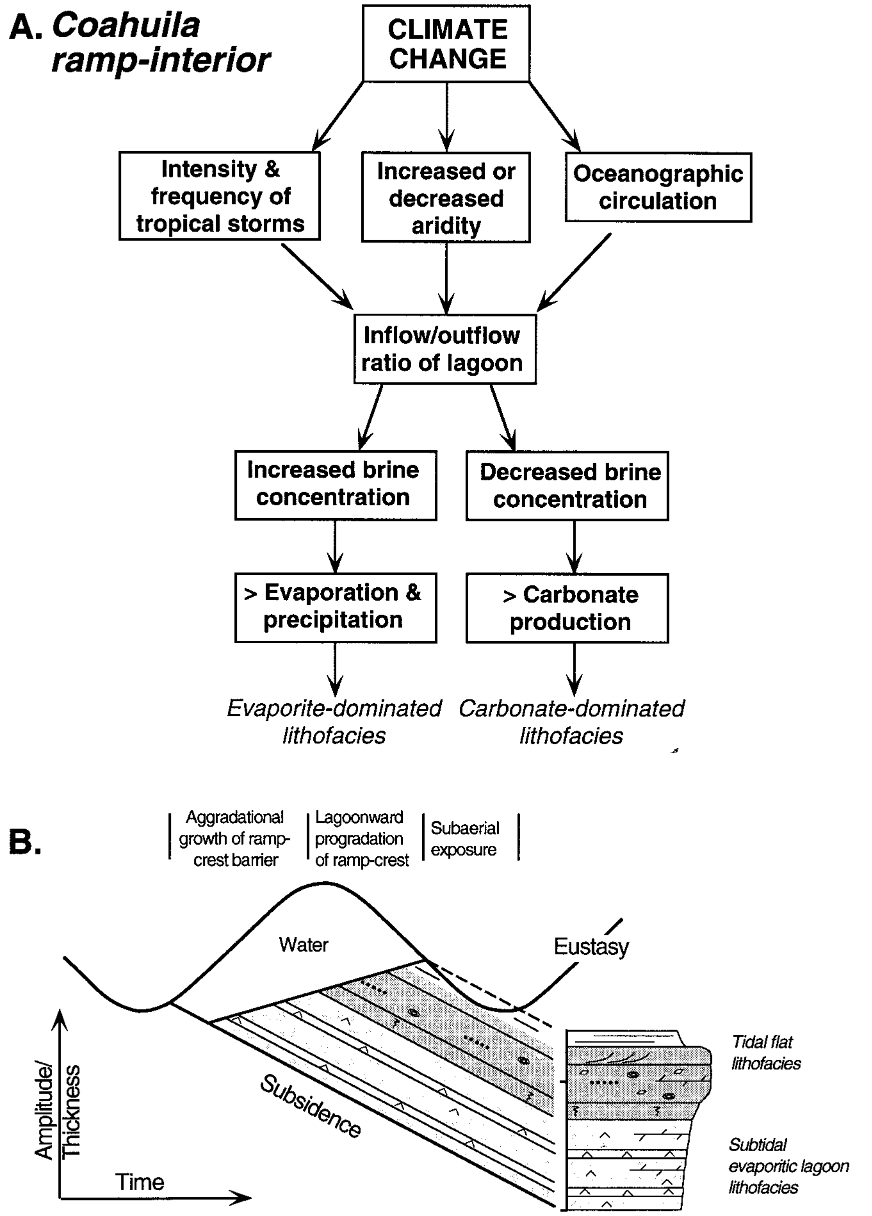

FIG. 11.—**A)** Simplified flow model illustrating the variety of environmental responses to global or regional climate change that may affect restricted platform lagoons such as the Coahuila ramp interior. The end result is cyclic deposition of evaporitic and carbonate lithofacies. **B)** Interplay between low-amplitude, high-frequency eustatic sea-level fluctuations and subsidence that creates accommodation space to form shallowing-upward evaporitic cycles of the Coahuila ramp interior. A symmetrical sine wave is used for simplicity and may not necessarily reflect the actual form of the eustatic signal during the Albian. The model does not imply any periodicities or sea-level amplitudes; accumulation rates of cycle lithofacies are assumed to be constant to simplify the model. These conceptual one-dimensional models are limited in that they illustrate only aggradational infilling, and we recognize that progradational migration of facies belts plays a critical role. (Adapted from ideas expressed in Read et al. 1986 and Osleger and Read 1991).

proposed a model whereby carbonate production by shallow-marine organisms decreases during cooler periods and increases during warmer periods. Inorganic precipitation would also be affected by changes in the solubility of $CaCO_3$ polymorphs with changes in ambient water temperature. In Hardie's model, the greater part of the deposition within individual peritidal cycles would occur during warm phases when carbonate production was high in the lagoonal ''factory'', with this sediment actively redistributed onto tidal flats (Fig. 12A). With cooling of the atmosphere–ocean system, aggradation and progradation would slow considerably and subsidence would take over as the dominant process, resulting in long-term nondeposition and progressive flooding of the tidal-flat cap. This model is difficult to test but should not be discounted as a potential influence on peritidal cycle generation, especially in concert with the abundant evidence for climatic control on surface productivity of Cretaceous open oceans and the resulting high-resolution pelagic record of cyclicity throughout the Tethys.

Eustasy.—Low-amplitude, high-frequency eustatic fluctuations are the likely primary control on the formation of up to 140 consecutive meter-scale peritidal cycles deposited on the Cupido carbonate shelf. The fundamental model relating eustatic sea-level fluctuations to the development of individual peritidal cycles has been extensively detailed in the literature (e.g., Grotzinger 1986; Koerschner and Read 1989; Goldhammer et al. 1990; Goldhammer et al. 1993; Osleger and Read 1991) and is diagramatically expressed in Figure 12B.

We suggest that eustatic fluctuations were of low amplitude, because slower rates of eustatic change accompanying low amplitudes would have permitted tidal flats to track sea level, resulting in cycles with relatively thin subtidal bases and thick intertidal caps (Read et al. 1986; Koerschner and Read 1989), similar to those formed on the Cupido carbonate platform. In contrast, a high-amplitude sea-level signal would have left tidal flats stranded and produced subtidal-dominated cycles capped by disconformities similar to those of the Plio-Pleistocene of Florida and the Bahamas (Perkins 1977; Beach and Ginsburg 1980). A minimum estimate of sea-level amplitude is given by the average cycle thickness, and thus we estimate 5–10 m as a reasonable minimum amplitude.

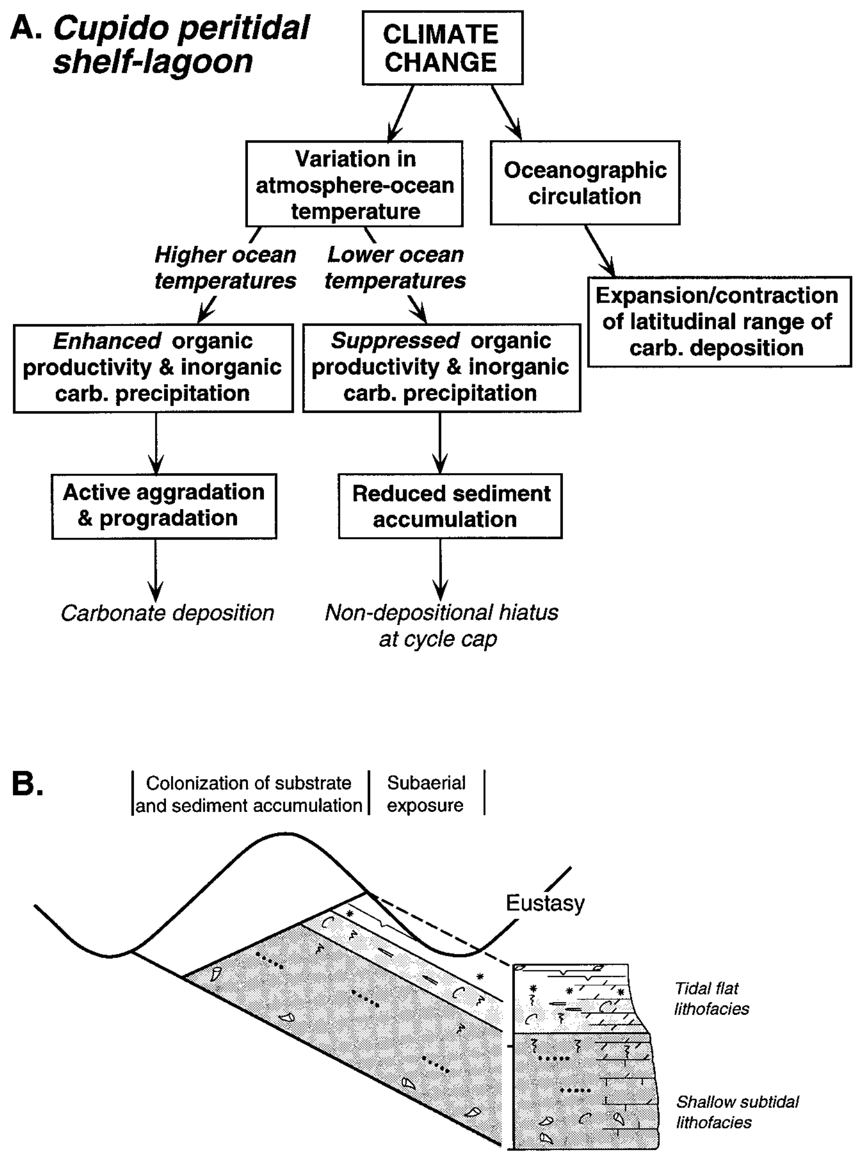

FIG. 12.—**A)** Simplified flow model illustrating the variety of environmental responses to global or regional climate change that may affect cyclic peritidal deposition such as dominates the Cupido shelf-lagoon. **B)** One-dimensional model for the formation of peritidal cycles illustrating the interplay between low-amplitude, high-frequency eustasy, subsidence, and sediment accumulation. Variables similar to model for evaporitic cycles illustrated in Figure 11. Perhaps the primary difference is the main process occurring during initial flooding. The nondepositional lag time in the evaporitic platform interior can be characterized by gradually increasing brine concentrations as the lagoon becomes more isolated by the upbuilding ramp-crest shoal keeping pace with rising sea level. In contrast, the nondepositional lag time in the peritidal belt may reflect the differential colonization of the substrate by carbonate-secreting organisms (Tipper 1997).

Autogenic Processes.—Broad-scale environmental changes, such as fluctuations in sea-surface temperature, salinity, availability of nutrients, predominant wind direction, and thermohaline circulation, exert regional influences on carbonate platform deposition (Schlager 1992, 1993). Changes in sediment supply governed by environmental factors should produce a spatial distribution of large-scale stratal geometries significantly different from those that relative sea-level changes alone would generate. For example, spatial differences in sediment distribution and accumulation have been observed in the Three Creeks area of Andros Island in the Bahamas, where tidal flats are currently prograding on the southwestern side of Andros but are backstepping on the northwestern side because of the dominant northwesterly winter storm track in the Bahamas (Gebelein 1974).

The influence of windward–leeward orientation of the Cupido shelf margin relative to dominant current, wave, and wind patterns may have exerted a critical autogenic control on margin composition and architecture across the interior shelf lagoon (Fig. 4A). The reefal Cupido margin flanking the eastern edge of the platform faced windward toward the open Gulf and likely experienced strong wave energy and high rates of biologic productivity, comparable to many modern east-facing reef margins (e.g., Bahamas, Belize, Great Barrier Reef). The southern shoal margin of the Cupido platform, oriented perpendicular to the open Gulf, may have been dominated by longshore currents and suppressed wave and wind energy, resulting in the south-to-southwest migration of sand shoals and general absence of organic buildups. These windward–leeward effects might have controlled the migration direction of tidal flats on the Cupido shelf lagoon. Peritidal cycles may be well developed in low-energy leeward settings where sediment accumulation exceeds sediment removal on tidal flats, resulting in progradational geometries. Conversely, in laterally adjacent environments facing major storm-track orientations, the balance may be tipped toward greater sediment removal, resulting in poorly developed peritidal cycles with thin or absent tidal-flat caps. This autogenic scenario can partially explain the difficulty in correlating individual cycles from one section to another on the Cupido platform (and many other Phanerozoic platforms).

Coahuila Deep-Platform ''Cycles''

Autogenic Processes.—Homogeneous mudstone and wackestone interspersed with firmgrounds and hardgrounds on the Coahuila deep ramp reflect the alternation of depositional and nondepositional episodes. The for-

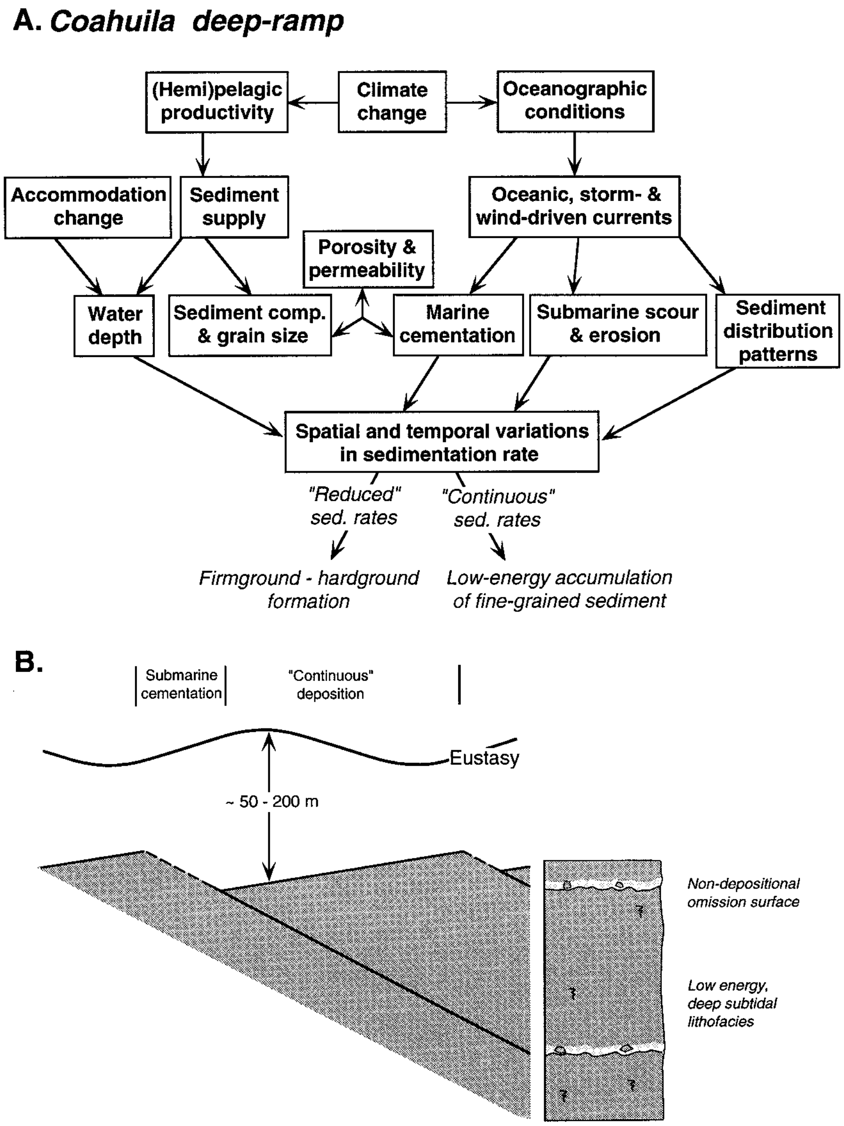

FIG. 13.—**A)** Simplified flow model of the variety of factors that interact to influence sedimentation rates on deep platforms (~ 50–200 m water depth) such as the Coahuila. **B)** One-dimensional model illustrating one example of how deep-ramp ''cycles'' of the Coahuila platform might be generated by eustasy. During the highest rates of sea-level rise, sedimentation rates are reduced in response to deepening, potentially resulting in submarine cementation and firm/hardground formation. Sedimentation resumes with the turnaround in sea level, resulting in deposition of homogeneous foraminiferal wackestones and lime mudstones.

mation of firmgrounds and hardgrounds is a common background process on many modern carbonate platforms (Bathurst 1971; Schlager and James 1978; Mullins et al. 1980; Betzler et al. 1995). They are generated under conditions of slow sedimentation that permit precipitation of submarine cements along the sediment–water interface. Water depth, sedimentation rate, temperature, organic productivity, sediment composition, petrophysical characteristics, and grain size are all important factors influencing the diagenetic potential of deep-water sediment (Schlanger and Douglas 1974; Kendall and Schlager 1981). In addition, oceanic currents, prevailing storm-track orientations, and trade-wind-driven currents all may contribute toward creating the right conditions for firmground/hardground formation. The Coahuila deep ramp (Upper Tamaulipas Formation) appears to have been an areally extensive region of low-energy, low-volume sedimentation with no apparent physiographic barriers separating it from the open ancestral Gulf (Fig. 4B). Oceanic currents or prevailing storm currents originating in the open Gulf could have swept unimpeded across the Coahuila deep ramp (~ 50–200 m deep), generating cemented surfaces in a random areal distribution, as well as randomly through time. The wide variety of interacting factors that control sedimentation rates on deep platforms is complex and generally unpredictable, so any model for cyclicity on deep platforms such as the Coahuila is inherently speculative (Fig. 13A).

Firmgrounds and hardgrounds may be traceable over thousands of square kilometers (Bromley and Gale 1982) or, conversely, may die out across a few tens to hundreds of meters (Wilson and Palmer 1992). The difficulty in correlating individual firmgrounds or hardgrounds between sections across the Coahuila deep ramp (Fig. 9B) illustrates the limited lateral distribution and suggests that their origin may simply be due to local, ambient environmental conditions. Firmgrounds and hardgrounds preferentially form on more permeable and porous sediment surfaces and can therefore be regarded as ''facies selective'' features (Kendall and Schlager 1981), suggesting that the spatial distribution of firmgrounds and hardgrounds may also be an artifact of the permeability characteristics of the substrate.

Eustasy.—Formation of firmgrounds and hardgrounds has been attributed to both rapid sea-level rises (Kendall and Schlager 1981; Sarg 1988; Fürsich et al. 1992) and sea-level falls (James and Bone 1991; Martire 1992; Eberli et al. 1995). Long-term rises lead to slow sedimentation rates and condensed sections in which firmgrounds and hardgrounds are abundant (Sarg 1988). During long-term falls, firmgrounds and hardgrounds form along the zone of wave abrasion near fair-weather or storm wave base where the substrate is swept clear of sediment and circulation of water through the sediment surface is enhanced (Osleger 1991; James and Bone 1991; Eberli et al. 1995). The firmgrounds and hardgrounds of the Coahuila

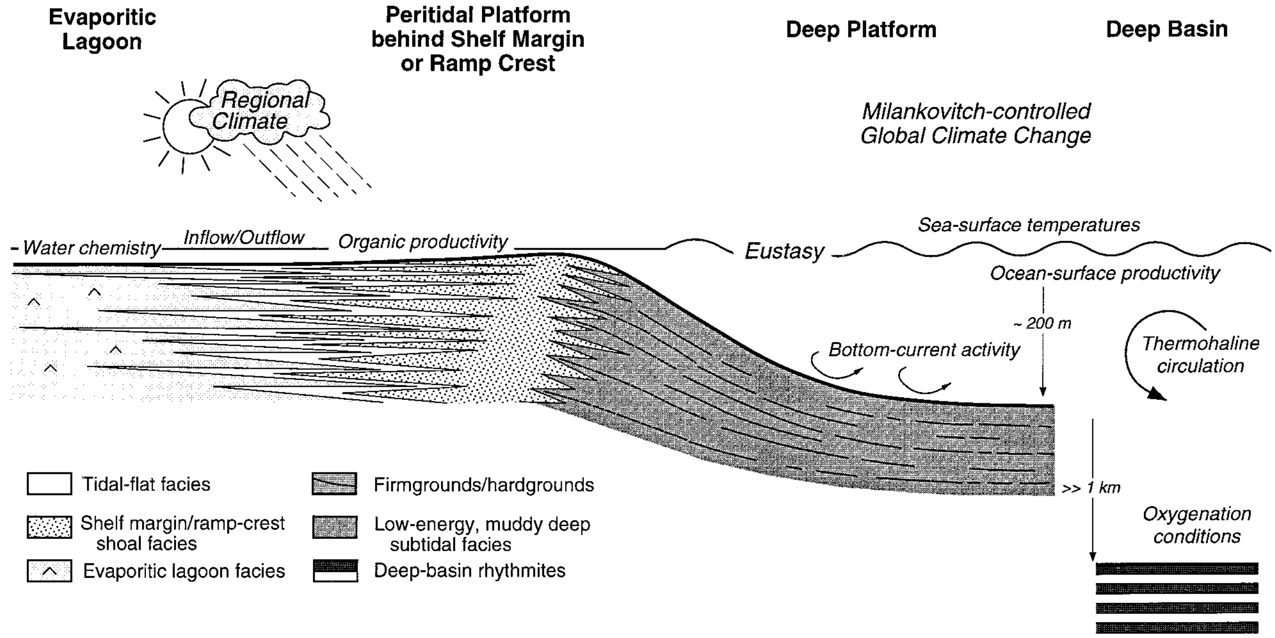

FIG. 14.—Schematic model illustrating the dominant variables acting upon a composite platform representing the three main paleoenvironmental settings of the Cupido and Coahuila shallow platforms. Also shown are critical processes operating contemporaneously in Tethyan deep basinal settings.

deep ramp might likewise have formed in response to high-frequency eustatic changes and attendant reduced sedimentation rates (Fig. 13B). The low-amplitude sea-level fluctuations of the Cretaceous greenhouse world would have changed the absolute water depth of the deep substrate only very slightly, however, relative to the estimated 50–200 m depths of the Coahuila deep ramp. These amplitudes may have been sufficient, however, to tip the balance between deposition and nondeposition in certain deep-ramp locations.

DEPOSITIONAL MODEL

The previous section on controlling mechanisms illustrates how climate change, autogenic processes, and eustasy may individually affect the generation of meter-scale cycles on the Cupido and Coahuila platforms (as well as other greenhouse platforms). The ideas and models presented in the previous discussion, constrained by the field data from the Cupido and Coahuila platforms, lead to an integrated, qualitative depositional model (Fig. 14) in which eustasy is the dominant allogenic control with a significant, but subordinate, overprint generated by regional climate change and autogenic processes. Additional indirect support for eustasy as the primary control on development of meter-scale cycles is provided by the scale-independent architecture of all genetic units, interpreted to reflect accommodation change at a range of temporal scales.

In essence, the schematic depositional model (Fig. 14) simplifies the two platforms into a single composite two-dimensional profile that illustrates how individual meter-scale cycles may develop in unique environmental settings during low-amplitude, high-frequency pulses of sea-level change. During each sea-level rise, the Cupido and Coahuila platform margins likely aggraded and narrowed, maintaining their vertical growth to match the newly generated accommodation. Tidal flats were constrained to a narrow belt in the lee of the margins, with subtidal conditions prevailing across the platform interiors. Deposition in the Cupido shelf lagoon during sea-level rise was characterized by a variety of shallow-subtidal carbonate lithofacies, whereas gypsiferous mudstones and massive gypsum dominated deposition in the Coahuila ramp interior. In the deep waters surrounding both platforms, sedimentation rates potentially decreased during sea-level rises to the point that omission surfaces locally developed on the sea floor.

With each individual episode of sea-level fall and consequent accommodation decrease, the Cupido and Coahuila platform margins prograded, accompanied by an expansion of the peritidal belt. Tidal-flat caps developed over subtidal carbonates on the Cupido shelf, whereas high-energy grainstones or tidal-flat laminates were deposited over evaporitic lithofacies in the Coahuila ramp interior. Cycle development was likely spatially variable, influenced by preexisting relief, differential subsidence, and the ambient environmental conditions across the broad platforms. Sub-basins filled with concentrated brines may have remained on the Coahuila ramp interior, precipitating evaporites coeval with prograding tidal flats. The Cupido shelf probably appeared as a mosaic of actively prograding tidal flats and adjacent subtidal lagoons during low-accommodation phases, perhaps because of storm-track orientation controlling the distribution of sediment. In the deep waters surrounding both platforms, muddy carbonates may have accumulated as hemipelagic sedimentation was enhanced by overproduction on the shallow platform and progradation of the platform margins, resulting in redistribution of sediment out to the deep platform.

Superimposed on the stratigraphic record of sea-level fluctuations are countless sedimentologic effects of autogenic environmental ''noise'' inherent to the depositional setting. As discussed, autogenic noise may be generated by variations in carbonate production and dispersal, intensity and frequency of tropical storms and monsoons, thermohaline circulation patterns, and ambient ocean chemistry and temperature, all potentially interacting in a series of feedback loops. This autogenic overprint on the stratigraphic record may be influenced by regional or global climate change. Whatever the precise connection, autogenic and climatic processes interacted to generate laterally variable physiographic and oceanographic conditions on the Cupido and Coahuila carbonate platforms, contributing to the lateral complexity of cycle distribution. The overall hierarchy of cyclicity recorded in these Cretaceous platforms exhibits clear evidence for accommodation change as the primary control, however, underlying the overprint of autogenic and climatic controls.

DISCUSSION

Cretaceous stratigraphic cyclicity is recognized in a spectrum of depositional settings. Compilations of published data on Cretaceous meter-scale

TABLE 5.—*Examples of Cretaceous hemipelagic and pelagic cycles*

Age	Location	Platform/Basin	Depositional Setting	Cycle Type	Suggested Mechanism	Reference
Campanian	South Atlantic	Rio Grande Rise	Pelagic	Carbonate-marl	Changes in productivity caused by climatic changes	Park et al. 1993
Campanian-early Maastrichtian	Northwest Australia	Exmouth Plateau	Pelagic	Chalk cycles	Climate changes	Boyd et al. 1994
Barremian-Cenomanian	Northern Italy	Southern Alps	Hemipelagic/pelagic	Limestone-marl	Climate changes	Claps and Maseti 1994
Barremian, Albian-Cenomanian	Italy	Umbrian-Marchean Basin	Pelagic	Limestone-marl	Productivity changes driven by Milankovitch-controlled climatic shifts	Herbert and Fischer 1986
Aptian-Albian	Italy	Umbrian-Marchean Basin	Pelagic	Limestone-marl	Dissolution/redox, productivity	de Boer 1982
Cenomanian	Italy	Central Apennines	Pelagic	Limestone-marl	Productivity changes	Schwarzacher 1994
Valanginian	Southeastern France	Vocontian Trough	Pelagic	Limestone-marl	Climatic and oceanographic changes	Giraud et al. 1995
Barremian	Southeastern France	Vocontian Trough	Platform and basin	Shallow-subtidal and hemipelagic	Climatic changes, glacio-eustasy	Quesne and Ferry 1995
Hauterivian-Barremian	Switzerland	Eastern Helvetic Platform	Deep shelf	Alternation of bioclastic and siliciclastic packstones/grainstones with marls	Changes in nutrient levels due to increased runoff	Funk et al. 1993
Upper Cretaceous	Southern England	Wessex Basin	Deep hemipelagic basin	Alternation of chalk, nodular chalk, omission surfaces, winnowed horizons, hardgrounds	Sea-level changes, variations in bottom current strength	Kennedy and Garrison 1975; R.O.C.C. 1986; Bottjer et al. 1986
Cenomanian	Western Europe	Western European Basins	Pelagic to hemipelagic	Carbonate-marl, variation in ichnofabric	Climatic changes	Gale 1995
Campanian	Mississippi, Alabama	Northern Gulf Coast	Deep shelf	Marl-limestone	Productivity changes caused by changes in salinity and nutrient levels	Bottjer et al. 1986
Cretaceous	Central U.S.	Western Interior Basin	Deep foreland basin	Changes in biota	Transgressive-regressive sea-level cycles	Kauffman 1977; Bottjer et al. 1986
Cenomanian-Turonian	Colorado	Western Interior Basin	Deep foreland basin	Limestone-marlstone/shale changes in benthic environment (ichnofabric)	Changes in oxygenation of bottom waters induced by paleo-climate and paleo-oceanography	Pratt 1984; Bottjer et al. 1986
Cenomanian-Turonian	Colorado	Western Interior Basin	Deep foreland basin	Limestone-marl/shale	Climatic changes	Barron et al. 1985; R.O.C.C. 1986; Bottjer et al. 1986
Latest Cenomanian-early Turonian	Kansas, Colorado, Utah	Western Interior Basin	Deep foreland basin	Limestone-shale, marlstone-shale	Climatic changes and tectonically induced fluctuations	Elder et al. 1994
Cenomanian-Turonian	Colorado	Western Interior Basin	Deep foreland basin	Alternation of chalk, black shale, and marl	Climatic forcing of changes in carbonate productivity, redox conditions, & siliciclastic supply	Ricken 1996
Earliest Turonian	Southern Utah	Western Interior Basin	Deep foreland basin	Limestone-marlstone/calcareous shale	Climatic changes in freshwater discharge and terrigenous sediment supply	Sethi and Leithold 1994
Cenomanian-Turonian	Colorado	Western Interior Basin	Deep foreland basin	Limestone-marl	Productivity changes	Sageman et al. 1997
Lower Cretaceous	Blake Bahama Basin, North Atlantic; Gulf of Mexico	Blake Bahama Basin, Gulf of Mexico	Pelagic	Limestone-marl	Climatic changes or eustatic changes	Cotillon 1987
Late Aptian-earliest Albian; Cenomanian-early Coniacian	Brazil	Sergipe Basin	Deep basin	Shale-marl; mudstone-marl	Climatic changes forcing productivity changes	Koutsoukos et al. 1993

cyclicity (Tables 4, 5) permit a broad subdivision into (1) shallow-subtidal, peritidal, and evaporitic cycles deposited in a variety of subenvironments on shallow carbonate platforms, and (2) hemipelagic and pelagic cycles deposited in foredeeps and deep ocean basins. Shallow-subtidal, peritidal, and evaporitic cycles are predominantly interpreted to have formed in response to relative sea-level fluctuations, usually driven by eustasy. This interpretation is typically based on the asymmetric, upward-shallowing arrangement of lithofacies within shallow-marine cycles, inferred to reflect an initial rapid increase in accommodation followed by a gradual and progressive decrease in accommodation.

Cretaceous hemipelagic and pelagic cycles are typified by (1) well-bedded chalk or limestone alternating with marl or shale, or (2) alternations of chalk, omission surfaces, and winnowed horizons. These deep-water cycles are generally considered to have been ultimately controlled by climate variations, frequently interpreted as Milankovitch-driven, that affect ocean-surface productivity, deep-marine oxygenation levels, bottom-current strength, and continental runoff of nutrient-rich sediment (references in Table 5; Fig. 14). Convincing evidence for the precession and eccentricity signals of Milankovitch orbital origin has been documented from studies of pelagic strata of Barremian to Cenomanian age in northern and central Italy (e.g., de Boer 1982; Herbert and Fischer 1986; Fischer et al. 1991; Herbert et al. 1995). The Aptian and Albian part of the Italian pelagic succession (Piobbico core) is coeval with both evaporitic and peritidal cycles of the Cupido and Coahuila platforms. The temporal overlap of both shallow-marine and deep-marine stratigraphic cyclicity across a large area of the world supports the presumption that climatic changes driven by orbital variations in the Milankovitch frequency band are recorded in shallow-marine as well as deep-marine depositional settings.

A significant problem exists, however, in generating eustatic oscillations, the primary control on cycle development on shallow carbonate platforms, by climatic change in greenhouse worlds when continental glaciers were absent. Combinations of climate-driven processes that affect sea level may be necessary to generate the minimum 5–10 m of estimated eustatic change required to form Cretaceous shallow-marine cycles.

(1) Thermal expansion and contraction of ocean water responding to global changes in sea-surface temperatures might cause geologically significant sea-level changes. An increase of 1°C throughout the water column would increase sea level by about 1 m (Donovan and Jones 1979). The dramatic decadal-scale changes recognized in the Quaternary ice record (Dansgaard et al. 1993), when surface temperature changes of 10–20° occurred over geologically instantaneous time spans, attest to the potential of rapid changes in the volume of ocean water and the resulting effects on sea level.

(2) Even though major continental glaciations were absent during the

Cretaceous (Barron 1983), small ice caps or alpine glaciers may have existed. Global falls in sea level seem to coincide with cooler temperatures recorded in oxygen isotopes of Cretaceous sedimentary rocks, which suggests that minor glaciations in the 10^5 year range existed during Cretaceous greenhouse time (Weissert and Lini 1991). Cretaceous dropstone deposits found in Australia, Arctic Canada, Siberia, and Alaska indicate that seasonal ice rafting existed (Frakes and Francis 1988). Melting of alpine glaciers and small ice caps has produced estimated sea-level rises of up to 5 cm within the last century (Meier 1984; Wigley and Raper 1987). Although these changes are relatively small and highly variable in the short term, when extrapolated to the 10^4 to 10^5 year range they might cause sea-level changes of several tens of centimeters to a few meters.

(3) Climate-driven changes in water storage volume in groundwater and lakes (e.g., monsoonal rainfall) have been calculated to potentially produce 2–8 m changes in sea level (Jacobs and Sahagian 1995). The Tethyan distribution of continents around the Cretaceous equator should have generated a monsoonal climate (Barron et al. 1995), and some of the remnant rift basins created during the breakup of Gondwana might have provided the necessary storage volume for increased seasonal rainfall.

Thus, some combination of thermal expansion and contraction of ocean water, waxing and waning of small ice caps and alpine glaciers, and changes in the storage capacity of aquifers and lakes, all governed by climatic changes and perhaps driven by Milankovitch rhythms, could collectively have generated the low-amplitude eustatic fluctuations proposed as the direct control on cyclostratigraphy of Lower Cretaceous platforms of northeastern Mexico.

CONCLUSIONS

(1) Meter-scale cycles occur in three different paleoenvironmental settings of the Lower Cretaceous Cupido (Barremian–Aptian) and Coahuila (Albian) carbonate platforms of northeastern Mexico: restricted evaporitic lagoon, peritidal shelf lagoon, and low-energy deep platform. These meter-scale cycles stack into intermediate-scale high-frequency sequences and large-scale composite sequences that can be correlated across the Cupido and Coahuila platforms. On the basis of similar vertical arrangements of lithofacies, these larger-scale genetic units are fundamentally macroscale versions of meter-scale cycles.

(2) Regional climate change, autogenic processes, and eustasy likely interact to generate laterally variable meter-scale cycles. The scale-independent architecture of all genetic units, interpreted to reflect a composite history of accommodation change, permits the inference that low-amplitude, high-frequency eustatic changes were the primary control on meter-scale cycle development. Thus, the qualitative depositional model proposed to explain cyclicity on the Cupido and Coahuila platforms is based upon eustasy as the dominant allogenic control with a significant, but subordinate, overprint generated by regional climate change and autogenic processes.

(3) Well-documented evidence from Barremian–Cenomanian pelagic cycles strongly indicates that Milankovitch-driven climatic changes operated during the Early Cretaceous. Contemporaneous shallow-marine cyclicity in several locations suggests that these climatic changes may have had globally widespread effects. We propose that Milankovitch-driven global climatic changes produced low-amplitude, high-frequency eustatic fluctuations through a combination of processes to produce meter-scale cycles across the Cupido and Coahuila carbonate platforms, and perhaps on other Lower Cretaceous shallow-marine platforms as well.

ACKNOWLEDGMENTS

We give our special thanks to James Lee Wilson and Bill Ward, who introduced us to the field area and discussed many of the findings of this paper. Wolfgang Stinnesbeck (Universidad Autónoma de Nuevo León) and Paul Enos (University of Kansas) also helped us to better understand the stratigraphy of northeastern Mexico. We are grateful to the late Dr. William Sliter (U.S.G.S., Menlo Park) and Dr. José Longoria (Florida International University) for identifying planktonic foraminifers, Dr. Annie Arnaud-Vanneau (University of Grenoble, France) for identifying benthonic foraminifers, Dr. Keith Young (University of Texas) for classifying ammonites, and Dr. Timothy Bralower (University of North Carolina) for identifying nannoconids. Scott Edwards, Raully Jones, and Brian Murtagh provided able field assistance. This paper benefited from careful reviews by James Lee Wilson, Bill Ward, and Peter Sadler, and JSR reviewers Mark Harris, Mike Grammar, and Gregor Eberli. Financial support was provided by grants from the University of California Institute for Mexico and the United States, American Association of Petroleum Geologists, Sigma Xi, Geological Society of America, and National Science Foundation Grant EAR-9417872.

REFERENCES

AIGNER, T.A., 1985, Storm Depositional Systems: Dynamic Stratigraphy in Modern and Ancient Shallow-Marine Sequences: Lecture Notes in Earth Sciences, Berlin, Springer-Verlag, 174 p.

ARNAUD, H.M., FLOOD, P.G., AND STRASSER, A., 1995, Resolution Guyot (Hole 866A, Mid-Pacific mountains): Facies evolution and sequence stratigraphy, *in* Winterer, E.L., Sager, W.W., Firth, J.V., and Sinton, J.M., eds., Proceedings of the Ocean Drilling Program, Scientific Results, Volume 143: College Station, Texas, p. 133–159.

ARNAUD-VANNEAU, A., AND ARNAUD, H.M., 1990, Hauterivian to lower Aptian carbonate shelf sedimentation and sequence stratigraphy in the Jura and northern Subalpine chains (southeastern France and Swiss Jura), *in* Tucker, M.E., Wilson, J.L., Crevello, P.D., Sarg, J.R., and Read, J.F., eds., Carbonate Platforms, Facies, Sequences and Evolution: International Association of Sedimentologists, Special Publication 9, p. 203–233.

BARRON, E.J., 1983, A warm, equable Cretaceous: The nature of the problem: Earth-Science Reviews, v. 19, p. 305–338.

BARRON, E.J., ARTHUR, M.A., AND KAUFFMAN, E.G., 1985, Cretaceous rhythmic bedding sequences: a plausible link between orbital variations and climate: Earth and Planetary Science Letters, v. 72, p. 327–340.

BARRON, E.J., FAWCETT, P.J., AND PETERSON, W.H., 1995, A ''simulation'' of mid-Cretaceous climate: Paleoceanography, v. 10, p. 953–962.

BARRON, E.J., HARRISON, C.G.A., SLOAN, J.L. II, AND HAY, W.W., 1981, Paleogeography, 180 million years ago to the present: Eclogae Geologicae Helvetiae, v. 74, p. 443–470.

BATHURST, R.G.C., 1971, Carbonate Sediments and Their Diagenesis: Amsterdam, Elsevier, Developments in Sedimentology 12, 658 p.

BEACH, D.K., AND GINSBURG, R.N., 1980, Facies succession of Plio-Pleistocene carbonates, northwestern Great Bahama Bank: American Association of Petroleum Geologists, Bulletin, v. 64, p. 1634–1642.

BERNER, R.A., 1994, Geocarb II: A revised model of atmospheric CO_2 over Phanerozoic time: American Journal of Science, v. 294, p. 56–91.

BETZLER, C., BRACHERT, T.C., AND KROON, D., 1995, Role of climate in partial drowning of the Queensland Plateau carbonate platform (northern Australia): Marine Geology, v. 123, p. 11–32.

BISHOP, B.A., 1970, Stratigraphy of Sierra de Picachos and vicinity, Nuevo Leon, Mexico: American Association of Petroleum Geologists, Bulletin, v. 54, p. 1245–1270.

BLOXSOM, W.E., 1972, A Lower Cretaceous (Comanchean) prograding shelf and associated environments of deposition, northern Coahuila, Mexico [unpublished Master's thesis]: University of Texas, Austin, 207 p.

BÖSE, E., 1927, Cretaceous ammonites from Texas and northern Mexico: University of Texas, Bulletin 2748, p. 143–357.

BOTTJER, D.J., ARTHUR, M.A., DEAN, W.E., HATTIN, D.E., AND SARDA, C.E., 1986, Rhythmic bedding produced in Cretaceous pelagic carbonate environments: sensitive recorder of climatic cycles: Paleoceanography, v. 1, p. 467–481.

BOYD, R., HUANG, Z., AND O'CONNELL, S., 1994, Milankovitch cyclicity in Late Cretaceous sediments from the Exmouth plateau of northwest Australia, *in* de Boer, P.L., and Smith, D.G., eds., Orbital Forcing and Cyclic Sequences: International Association of Sedimentologists, Special Publication 19, p. 145–166.

BROMLEY, R.G., 1975, Trace fossils at omission surfaces, *in* Frey, R.W., ed., The Study of Trace Fossils; A Synthesis of Principles, Problems, and Procedures in Ichnology: New York, Springer-Verlag, p. 399–428.

BROMLEY, R.G., AND GALE, A.S., 1982, The lithostratigraphy of the English Chalk Rock: Cretaceous Research, v. 3, p. 273–306.

BURROWS, R.H., 1909, Geology in northern Mexico: Mining and Scientific Press, v. 99, p. 290–294.

CANTÚ CHAPA, C.M., SANDOVAL, R., AND ARENAS, R., 1985, Evolución sedimentaria del Cretácico inferior en el norte de México: Instituto Mexicano del Petróleo, Revista, v. 17, p. 14–37.

CANTWELL, W.A., AND WARD, W.C., 1990, Shelf-to-basin lithofacies transition between the Aurora and Upper Tamaulipas Formations and its relationship to postulated early Mesozoic transcurrent faults (abstract): Geological Society of America, Annual Meeting, Dallas, Texas, Abstracts with Programs, p. 185.

CERLING, T.E., 1991, Carbon dioxide in the atmosphere: evidence from Cenozoic and Mesozoic paleosols: American Journal of Science, v. 291, p. 377–400.

CHARLESTON, S., 1974, Stratigraphy, tectonics, and hydrocarbon potential of the Lower Cretaceous, Coahuila Series, Coahuila, Mexico [unpublished Ph.D. thesis]: University of Michigan, Ann Arbor, 268 p.

CLAPS, M., AND MASETTI, D., 1994, Milankovitch periodicities recorded in the Cretaceous deep-sea sequences from the southern Alps (northern Italy), *in* de Boer, P.L., and Smith, D.G., eds., Orbital Forcing and Cyclic Sequences: International Association of Sedimentologists, Special Publication 19, p. 99–107.

Conklin, J., and Moore, C., 1977, Paleoenvironmental analysis of the Lower Cretaceous Cupido Formation, northeast Mexico, *in* Bebout, D.G., and Loucks, R.G., eds., Cretaceous Carbonates of Texas and Mexico: The University of Texas, Bureau of Economic Geology, Report of Investigations no. 89, p. 302–323.

Cotillon, P., 1987, Bed-scale cyclicity of pelagic Cretaceous successions as a result of world-wide control: Marine Geology, v. 78, p. 109–123.

Dansgaard, W., Johnsen, S.J., Clausen, H.B., Dahl-Jensen, D., Gundestrup, N.S., Hammer, C.U., Hvidberg, C.S., Steffensen, J.P., Sveinbjörnsdottir, A.E., Jouzel, J., and Bond, G., 1993, Evidence for general instability of past climate from a 250-kyr ice-core record: Nature, v. 364, p. 218–220.

Davis, G.R., and Nassichuk, 1975, Subaqueous evaporites of the Carboniferous Otto Fiord Formation, Canadian Arctic Archipelago: A summary: Geology, v. 3, p. 273–278.

de Boer, P.L., 1982, Cyclicity and the storage of organic matter in Middle Cretaceous pelagic sediments, *in* Einsele, G., and Seilacher, A., eds., Cyclic and Event Stratification: Berlin, Springer-Verlag, p. 456–475.

de Cisneros, C.J., and Vera, J.A., 1993, Milankovitch cyclicity in Purbeck peritidal limestones of the Prebetic (Berriasian, southern Spain): Sedimentology, v. 40, p. 513–537.

de Cserna, Z., 1956, de la Sierra Madre Oriental de México, entre Torreon y Monterrey: XX Congreso Geológico International, Mexico, 87 p.

Donovan, D.T., and Jones, E.J., 1979, Causes of world-wide changes in sea level: Geological Society of London, Journal, v. 136, p. 187–192.

Eberli, G.P., Bernoulli, D., Sanders, D., and Vescei, A., 1993, From aggradation to progradation: The Maiella platform, Abruzzi, Italy, *in* Simo, J.A., Scott, R.W., and Masse, J.-P., eds., Cretaceous Carbonate Platforms: American Association of Petroleum Geologists, Memoir 56, p. 213–232.

Eberli, G.P., Warzeski, E.R., Ginsburg, R.N., Anselmetti, F.S., and Kenter, J.A.M., 1995, The record of sea level controlled sedimentation in lithology, logs and seismic data, Late Cenozoic, Great Bahama Bank (abstract): American Association of Petroleum Geologists, Annual Convention, Houston, Abstracts with Programs, p. 25A.

Elder, W.P., Gustason, E.R., and Sageman, B.B., 1994, Correlation of basinal carbonate cycles to nearshore parasequences in the Late Cretaceous Greenhorn seaway, Western Interior U.S.A.: Geological Society of America, Bulletin, v. 106, p. 892–902.

Elliot, L.A., and Warren, J.K., 1989, Stratigraphy and depositional environment of the Lower San Andres Formation in the subsurface and equivalent outcrops: Chavez, Lincoln, and Roosevelt Counties: American Association of Petroleum Geologists, Bulletin, v. 73, p. 1307–1325.

Elliot, T.L., 1979, Deposition and diagenesis of carbonate slope deposits, Lower Cretaceous, northeastern Mexico [unpublished Ph.D. thesis]: University of Texas, Austin, 330 p.

Fischer, A.G., Herbert, T.D., Napoleone, G., Premoli Silva, I., and Ripepe, M., 1991, Albian pelagic rhythms: Journal of Sedimentary Petrology, v. 61, p. 1164–1172.

Frakes, J.R., and Francis, M.N., 1988, A guide to Phanerozoic cold polar climates from high-latitude ice-rafting in the Cretaceous: Nature, v. 333, p. 547–549.

Freeman, K.H., and Hayes, J.M., 1992, Fractionation of carbon isotopes by phytoplankton and estimates of ancient CO_2 levels: Global Biogeochemical Cycles, v. 6, p. 185–198.

Fuentes, R.P., 1964, Stratigraphy of Sierra Santa Clara and Sierra Gomas, Nuevo Leon, Mexico [unpublished M.S. thesis]: University of Texas, Austin, 216 p.

Funk, H., Föllmi, K.B., and Mohr, H., 1993, Evolution of the Tithonian–Aptian carbonate platform along the northern Tethyan margin, eastern Helvetic Alps, *in* Simo, J.A., Scott, R.W., and Masse, J.-P., eds., Cretaceous Carbonate Platforms: American Association of Petroleum Geologists, Memoir 56, p. 387–407

Fürsich, F.T., 1979, Genesis, environments, and ecology of Jurassic hardgrounds: Neues Jahrbuch für Geologie und Paläontologie, Abhandlungen, v. 158, p. 1–63.

Fürsich, F.T., Oschmann, W., Singh, I.B., and Jaitly, A.K., 1992, Hardgrounds, reworked concretion levels and condensed horizons in the Jurassic of western India: their significance for basin analysis: Geological Society of London, Journal, v. 149, p. 313–331.

Gale, A.S., 1995, Cyclostratigraphy and correlation of the Cenomanian Stage in western Europe, *in* House, M.R., and Gale, A.S., eds., Orbital Forcing Timescale and Cyclostratigraphy: Geological Society of London, Special Publication 85, p. 177–197.

García, A., Segura, M., García-Hidalgo, J.F., and Carenas, B., 1993, Mixed siliciclastic and carbonate platform of Albian–Cenomanian age of the Iberian basin, Spain, *in* Simo, J.A., Scott, R.W., and Masse, J.-P., eds., Cretaceous Carbonate Platforms: American Association of Petroleum Geologists, Memoir 56, p. 255–269.

García, A., Segura, M., and García-Hidalgo, J.F., 1996, Sequences, cycles and hiatuses in the Upper Albian–Cenomanian of the Iberian Ranges (Spain): a cyclostratigraphic approach: Sedimentary Geology, v. 103, p. 175–200.

Garza, G.R., 1973, Model sedimentario del Albiano–Cenomaniano en la porción sureste de la plataforma de Coahuila (Prospecto Parras, Edo. de Coahuila): Asociación Mexicana de Geólogos Petroleros, Boletín, v. 25, p. 300–339.

Gebelein, C.D., 1974, Guidebook for modern Bahamian platform environments: Geological Society of America, Annual Meeting, Field Trip Guide, 93 p.

Giraud, F., Beaufort, L., and Cotillon, P., 1995, Periodicities of carbonate cycles in the Valanginian of the Vocontian Trough: a strong obliquity control, *in* House, M.R., and Gale, A.S., eds., Orbital Forcing Timescale and Cyclostratigraphy: Geological Society of London, Special Publication 85, p. 143–164.

Goldhammer, R.K., Dunn, P.A., and Hardie, L.A., 1990, Depositional cycles, composite sea-level changes, cycle stacking patterns, and the hierarchy of stratigraphic forcing: Examples from Alpine Triassic platform carbonates: Geological Society of America, Bulletin, v. 102, p. 535–562.

Goldhammer, R.K., Lehmann, P.J., and Dunn, P.A., 1993, The origin of high frequency platform carbonate cycles and third-order sequences (Lower Ordovician El Paso Gp, west Texas): Constraints from outcrop data and stratigraphic modeling: Journal of Sedimentary Petrology, v. 63, p. 318–359.

Goldhammer, R.K., Lehmann, P.J., Todd, R.G., Wilson, J.L., Ward, W.C., and Johnson, C.R., 1991, Sequence Stratigraphy and Cyclostratigraphy of the Mesozoic of the Sierra Madre Oriental, Northeast Mexico, A Field Guidebook: SEPM, Gulf Coast Section, 85 p.

Grötsch, J., 1994, Guilds, cycles and episodic vertical aggradation of a reef (late Barremian to early Aptian, Dinaric carbonate platform, Slovenia), *in* de Boer, P.L., and Smith, D.G., eds., Orbital Forcing and Cyclic Sequences: International Association of Sedimentologists, Special Publication 19, p. 227–242.

Grötsch, J., 1996, Cycle stacking and long-term sea level history in the Lower Cretaceous (Gavrovo Platform, NW Greece): Journal of Sedimentary Research, v. 66, p. 723–736.

Grötsch, J., Schroeder, R., Noe, S., and Flügel, E., 1993, Carbonate platforms as recorders of high-amplitude eustatic sea-level fluctuations: The Late Albian *appenninica*-event: Basin Research, v. 5, p. 197–212.

Grotzinger, J.P., 1986, Cyclicity and paleoenvironmental dynamics, Rocknest platform, northwest Canada: Geological Society of America, Bulletin, v. 97, p. 1208–1231.

Handford, C.R., 1991, Chapter 1, Marginal marine halite, *in* Melvin, J.L., ed., Evaporites, Petroleum and Mineral Resources: Amsterdam, Elsevier, Developments in Sedimentology 50, p. 1–66.

Hardie, L.A., 1986, Stratigraphic models for carbonate tidal flat deposition: *in* Hardie, L.A., and Shinn, E.A., Carbonate Depositional Environments, Modern and Ancient: Part 3: Tidal Flats: Colorado School of Mines Quarterly, v. 81, p. 59–74.

Herbert, T.D., and Fischer, A.G., 1986, Milankovitch climatic origin of mid-Cretaceous black shale rhythms in central Italy: Nature, v. 321, p. 739–743.

Herbert, T.D., Premoli Silva, I., Erba, E., and Fischer, A.G., 1995, Orbital chronology of Cretaceous–Paleocene marine sediments, *in* Berggren, W.A., Kent, D.V., Aubry, M.-P., and Hardenbol, J., eds., Geochronology, Time Scales and Global Stratigraphic Correlation: SEPM, Special Publication 54, p. 81–93.

Hovorka, S.D., 1987, Depositional environments of marine-dominated halite, Permian San Andres Formation, Texas: Sedimentology, v. 34, p. 1029–1054.

Huber, B.T., Hodell, D.A., and Hamilton, C.P., 1995, Middle–late Cretaceous climate of the southern high latitudes: Stable isotopic evidence for minimal equator-to-pole thermal gradients: Geological Society of America, Bulletin, v. 107, p. 1164–1191.

Humphrey, W.E., 1949, Geology of the Sierra de los Muertos area, Mexico (with descriptions of Aptian Cephalopods from the La Peña Formation): Geological Society of America, Bulletin, v. 60, p. 89–176.

Hunt, D., and Tucker, M.E., 1993, The middle Cretaceous Urgonian platform of southeastern France, *in* Simo, J.A., Scott, R.W., and Masse, J.-P., eds., Cretaceous Carbonate Platforms: American Association of Petroleum Geologists, Memoir 56, p. 409–453.

Imlay, R.W., 1936, Evolution of the Coahuila Peninsula, Mexico, part 4, Geology of the western part of the Sierra de Parras: Geological Society of America, Bulletin, v. 47, p. 1091–1152.

Imlay, R.W., 1937, Geology of the middle part of the Sierra de Parras, Coahuila, Mexico: Geological Society of America, Bulletin, v. 48, p. 587–630.

Imlay, R.W., 1938, Studies of the Mexican Geosyncline: Geological Society of America, Bulletin, v. 49, p. 1651–1694.

Imlay, R.W., 1944a, Cretaceous formations of central America and Mexico: American Association of Petroleum Geologists, Bulletin, v. 28, p. 1077–1195.

Imlay, R.W., 1944b, Correlations of the Cretaceous formations of the Greater Antilles, central America, and Mexico: Geological Society of America, Bulletin, v. 55, p. 1005–1046.

Jacobs, D.K., and Sahagian, D.L., 1995, Milankovitch fluctuations in sea level and recent trends in sea-level change: Ice may not always be the answer, *in* Haq, B.U., ed., Sequence Stratigraphy and Depositional Response to Eustatic, Tectonic and Climatic Forcing: Dordrecht, The Netherlands, Kluwer, p. 329–366.

James, N.P., and Bone, Y., 1991, Origin of a deep cool water Oligo-Miocene limestone, Eucla Platform, Australia: Sedimentology, v. 38, p. 323–341.

Kauffman, E.G., 1977, Geological and biological overview—Western Interior Cretaceous basin, *in* Kauffman, E.G., ed., Cretaceous Facies, Faunas, and Paleoenvironments across the Western Interior Basin, Field Guide, North American Geological Convention II: Mountain Geologist, v. 13, no. 3 and 4, p. 75–99.

Kellum, L.B., Imlay, R.W., and Kane, W.G., 1936, Evolution of the Coahuila Peninsula, Mexico, Part 1, Relation of structure, stratigraphy and igneous activity to an early continental margin: Geological Society of America, Bulletin, v. 47, p. 969–1008.

Kelly, W.A., 1936, Evolution of the Coahuila Peninsula, Mexico, part 2, Geology of the mountains bordering the valleys of Acatita and Las Delicias: Geological Society of America, Bulletin, v. 47, p. 1009–1038.

Kendall, A.C., 1988, Aspects of evaporite basin stratigraphy, *in* Schreiber, B.C., ed., Evaporites and Hydrocarbons: New York, Columbia University Press, p. 11–65.

Kendall, A.C., 1992, Evaporites, *in* Walker, R.G., and James, N.P., eds., Facies Models: Response to Sea Level Change: Geological Association of Canada, p. 375–409.

Kendall, C.G.St.C., and Schlager, W., 1981, Carbonates and relative sea level change: Marine Geology, v. 44, p. 181–212.

Kennedy, W.J., and Garrison, R.E., 1975, Morphology and genesis of nodular chalks and hardgrounds in the upper Cretaceous of southern England: Sedimentology, v. 22, p. 311–386.

Kindred, F.R., 1988, Origin and diagenesis of carbonate mudstone, Aurora Formation (Lower Cretaceous), Coahuila, Mexico [unpublished Master's thesis]: University of New Orleans, 77 p.

Koerschner, W.F., and Read, J.F., 1989, Field and modelling studies of carbonate cycles, Virginia Appalachians: Journal of Sedimentary Petrology, v. 59, p. 654–687.

Koutsoukos, E.A.M., Destro, N., de Azambuja Filho, N.C., and Spadini, A.R., 1993, Upper Aptian–lower Coniacian carbonate sequences in the Sergipe basin, Northeastern Brazil, *in*

Simo, J.A., Scott, R.W., and Masse, J.-P., eds., Cretaceous Carbonate Platforms: American Association of Petroleum Geologists, Memoir 56, p. 127–144.

Krutak, P.R., 1967, Structural geology of the Sierra de la Gavia, Coahuila, Mexico: Geological Society of America, Bulletin, v. 78, p. 59–76.

Lehmann, C., 1997, Sequence stratigraphy and platform evolution of Lower Cretaceous (Barremian–Albian) carbonates of northeastern Mexico [unpublished Ph.D. thesis]: University of California, Riverside, 261 p.

Logan, B.W., 1987, The MacLeod Evaporite Basin, Western Australia: American Association of Petroleum Geologists, Memoir 44, 140 p.

Longo, G., D'Argenio, B., Ferreri, V., and Iorio, M., 1994, Fourier evidence for high-frequency astronomical cycles recorded in Early Cretaceous carbonate platform strata, Monte Maggiore, southern Apennines, Italy, *in* de Boer, P.L., and Smith, D.G., eds., Orbital Forcing and Cyclic Sequences: International Association of Sedimentologists, Special Publication 19, p. 77–85.

Longoria, J.F., 1984, Cretaceous biochronology from the Gulf of Mexico region based on planktonic microfossils: Micropaleontology, v. 30, p. 225–242.

Longoria, J.F., and Gamper, M.A., 1977, Albian planktonic foraminifera from the Sabinas Basin of northern Mexico: Journal of Foraminiferal Research, v. 7, p. 196–215.

Longoria, J.F., and Monreal, R., 1991, Lithostratigraphy, microfacies, and depositional environments of the Mesozoic of Sierra La Nieve, Coahuila, northeast Mexico: Sociedad Geológica de España, Revista, v. 4, p. 7–31.

Loucks, R.G., and Longman, M.W., 1982, Lower Cretaceous Ferry Lake Anhydrite, Fairway field, east Texas; product of shallow-subtidal deposition, *in* Depositional and Diagenetic Spectra of Evaporites—A Core Workshop: Society of Economic Paleontologists and Mineralogists, Core Workshop No. 3, p. 276–304.

Martín-Chivelet, J., and Giménez, R., 1992, Paleosols in microtidal sequences: Sierra de Utiel Formation, Upper Cretaceous, SE Spain: Sedimentary Geology, v. 81, p. 125–145.

Martire, L., 1992, Sequence stratigraphy and condensed pelagic sediments: An example from the Rosso Ammonitico Veronese, northeastern Italy: Palaeogeography, Palaeoclimatology, Palaeoecology, v. 94, p. 169–191.

McFarlan, E., Jr., and Menes, L.S., 1991, Lower Cretaceous, *in* Salvador, A., ed., The Geology of North America, Vol. J, The Gulf of Mexico Basin: The Geological Society of America, p. 181–204.

Meier, M.F., 1984, Contribution of small glaciers to global sea level: Science, v. 226, p. 1418–1421.

Minero, C.J., 1988, Sedimentation and diagenesis along open and island-sheltered platform margin, El Abra Formation, Cretaceous of Mexico, *in* James, N.P., and Choquette, P., eds., Paleokarst: New York, Springer-Verlag, p. 385–405.

Minero, C.J., 1991, Sedimentation and diagenesis along an island-protected windward carbonate platform margins of the Cretaceous El Abra Formation, Mexico: Sedimentary Geology, v. 71, p. 261–288.

Mitchum, R.M., Jr., and Van Wagoner, J.C., 1991, High-frequency sequences and their stacking patterns: sequence stratigraphic evidence of high-frequency eustatic cycles, *in* Biddle K.T., and Schlager, W., eds., The Record of Sea-Level Fluctuations: Sedimentary Geology, v. 70, p. 131–160.

Morán-Zenteno, D.J., 1994, The Geology of the Mexican Republic: American Association of Petroleum Geologists, Studies in Geology 39, 160 p.

Mullins, H.T., Neumann, A.C., Wilber, R.J., and Boardman, M.R., 1980, Nodular carbonate sediment on Bahamian slopes: possible precursors to nodular limestones: Journal of Sedimentary Petrology, v. 50, p. 117–131.

Mutti, M., and Weissert, H., 1995, Triassic monsoonal climate and its signature in Ladinian–Carnian carbonate platforms (southern Alps, Italy): Journal of Sedimentary Research, v. B65, p. 357–367.

Obradović, J., Mirković, M., Čadenović, D., and Djurdjević, J., 1993, Characteristics of the Cretaceous Periadriatic platforms of the Montenegrin littoral, Yugoslavia, *in* Simo, J.A., Scott, R.W., and Masse, J.-P., eds., Cretaceous Carbonate Platforms: American Association of Petroleum Geologists, Memoir 56, p. 233–241.

Osleger, D.A., 1991, Subtidal carbonate cycles: Implications for allocyclic vs. autocyclic controls: Geology, v. 19, p. 917–920.

Osleger, D.A., and Read, J.F., 1991, Relation of eustasy to stacking patterns of Late Cambrian cyclic carbonates: A field and computer modelling study: Journal of Sedimentary Petrology, Special Issue on Milankovitch Cyclicity, v. 61, p. 1225–1252.

Park J., and Oglesby, R.J., 1991, Milankovitch rhythms in the Cretaceous—GCM modelling study: Global and Planetary Change, v. 4, p. 329–355.

Park, J., D'Hondt, S.L., King, J.W., and Gibson, C., 1993, Late Cretaceous precessional cycles in double time: A warm-earth Milankovitch response: Science, v. 261, p. 1431–1434.

Parrish, J.T., 1993, Climate of the supercontinent Pangea: Journal of Geology, v. 101, p. 215–233.

Perkins, R.D., 1977, Pleistocene depositional framework of south Florida, *in* Enos, P., and Perkins, R.D., eds., Quaternary Sedimentation in South Florida: Geological Society of America, Memoir 147, p. 131–198.

Pirrie, D., Doyle, P., Marshall, J.D., and Ellis, G., 1995, Cooler Cretaceous climates: new data from the Albian of Western Australia: Geological Society of London, Journal, v. 125, p. 739–742.

Pratt, B.R., James, N.P., and Cowan, C.A., 1992, Peritidal carbonates, *in* Walker, R.G., and James, N.P., eds., Facies Models: Response to Sea Level Change: Geological Association of Canada, p. 303–322.

Pratt, L.M., 1984, Influence of paleoenvironmental factors on preservation of organic matter in Middle Cretaceous Greenhorn Formation, Pueblo, Colorado: American Association of Petroleum Geologists, Bulletin, v. 68, p. 1146–1159.

Purser, B.H., 1969, Syn-sedimentary marine lithification of Middle Jurassic limestones in the Paris Basin: Sedimentology, v. 12, p. 205–330.

Quesne, D., and Ferry, S., 1995, Detailed relationships between platform and pelagic carbonates (Barremian, SE France), *in* House, M.R., and Gale, A.S., eds., Orbital Forcing Timescales and Cyclostratigraphy: Geological Society of London, Special Publication 85, p. 165–176.

Read, J.F., Grotzinger, J.P., Bova, J.A., and Koerschner, W.F., 1986, Models for generation of carbonate cycles: Geology, v. 14, p. 107–110.

Research on Cretaceous Cycles (R.O.C.C.) Group, 1986, Rhythmic bedding in Upper Cretaceous pelagic carbonate sequences: Varying sedimentary response to climatic forcing: Geology, v. 14, p. 153–156.

Ricken, W., 1996, Bedding rhythms and cyclic sequences as documented in organic carbon–carbonate patterns, Upper Cretaceous, Western Interior, U.S.: Sedimentary Geology, v. 102, p. 131–154.

Röhl, U., and Ogg, J.G., 1996, Aptian–Albian sea level history from guyots in the western Pacific: Paleoceanography, v. 11, p. 595–624.

Ross, M.A., 1981, Stratigraphy of the Tamaulipas Limestone, Lower Cretaceous, Mexico, *in* Smith, C.I., ed., Lower Cretaceous Stratigraphy and Structure, Northern Mexico: West Texas Geological Society, Publication 81–74, p. 43–54.

Ruzyla, K., and Friedman, G.M., 1985, Factors controlling porosity in dolomite reservoirs of the Ordovician Red River Formation, Cabin Creek field, Montana, *in* Roehl, P.O., and Choquette, P.W., eds., Carbonate Petroleum Reservoirs: A Case Book: New York, Springer-Verlag, p. 39–58.

Sageman B.B., Rich, J., Arthur, M.A., Birchfield, G.E., and Dean W.E., 1997, Evidence for Milankovitch periodicities in Cenomanian–Turonian lithologic and geochemical cycles, Western Interior U.S.A.: Journal of Sedimentary Research, v. 67, p. 286–302.

Sarg, J.F., 1981, Petrology of the carbonate–evaporite facies transition of the Seven Rivers Formation (Guadalupian, Permian), southeast New Mexico: Journal of Sedimentary Petrology, v. 51, p. 73–96.

Sarg, J.F., 1988, Carbonate sequence stratigraphy, *in* Wilgus, C.K., Hastings, B.S., Kendall, C.G.St.C., Posamentier, H.W., Ross, C.A., and Van Wagoner, J.C., eds., Sea Level Changes: An Integrated Approach: SEPM, Special Publication 42, p. 155–181.

Schlager, W., 1992, Sedimentology and sequence stratigraphy of reefs and carbonate platforms, a short course: American Association of Petroleum Geologists, Continuing Education Course Note Series, no. 34, 71 p.

Schlager, W., 1993, Accommodation and supply—a dual control on stratigraphic sequences: Sedimentary Geology, v. 86, p. 111–136.

Schlager, W., and James, N.P., 1978, Low-magnesian calcite limestone forming at the deep-sea floor, Tongue of the Ocean, Bahamas: Sedimentology, v. 25, p. 675–702.

Schlanger, S.O., and Douglas, R.G., 1974, The pelagic ooze–chalk–limestone transition and its implication for marine stratigraphy, *in* Hsü, K.J., and Jenkyns, H.C., eds., Pelagic Sediments: On Land and under the Sea: International Association of Sedimentologists, Special Publication 1, p. 117–148.

Schwarzacher, W., 1994, Cyclostratigraphy of the Cenomanian in the Gubbio district, Italy, a field study, *in* de Boer, P.L., and Smith, D.G., eds., Orbital Forcing and Cyclic Sequences: International Association of Sedimentologists, Special Publication 19, p. 87–97.

Schwarzacher, W., and Fischer, A.G., 1982, Limestone–shale bedding and perturbations in the Earth's orbit, *in* Einsele, G., and Seilacher, A., eds., Cyclic and Event Stratification: Berlin, Springer-Verlag, p. 72–95.

Segura, M., García-Hidalgo, J.F, Carenas, B., and García, A., 1993, Late Cenomanian–early Turonian platform from central eastern Iberia, Spain, *in* Simo, J.A., Scott, R.W., and Masse, J.-P., eds., Cretaceous Carbonate Platforms: American Association of Petroleum Geologists, Memoir 56, p. 283–296.

Sellwood, B.W., Price, G.D., and Valdes, P.J., 1994, Cooler estimates for Cretaceous temperatures: Nature, v. 370, p. 453–455.

Sethi, P.S., and Leithold, E.L., 1994, Climatic cyclicity and terrigenous sediment influx to the early Turonian Greenhorn sea, southern Utah: Journal of Sedimentary Research, v. B64, p. 16–39.

Shinn, E.A., 1983, Tidal flat environments, *in* Scholle, P.A., Bebout, D.G., and Moore, C.H., eds., Depositional Environments in Carbonate Rocks: American Association of Petroleum Geologists, Memoir 33, p. 172–210.

Sliter, W.V., 1995, Cretaceous planktonic foraminifers from Sites 865, 866, and 869: A synthesis of Cretaceous pelagic sedimentation in the central Pacific Ocean basin, *in* Winterer, E.L., Sager, W.W., Firth, J.V., and Sinton, J.M., eds., Proceedings of the Ocean Drilling Program, Scientific Results, Volume 143: College Station, Texas, p. 15–30,

Strasser, A., 1988, Shallowing-upward sequences in Purbeckian peritidal carbonates (lowermost Cretaceous Swiss and French Jura Mountains): Sedimentology, v. 35, p. 369–383.

Tinker, S.W., 1985, Lithostratigraphy and biostratigraphy of the Aptian La Peña formation, northeast Mexico and South Texas (Part 1), and The depositional setting of the Aptian Pearsall–La Peña Formations, Texas subsurface and northeast Mexico: Why is there not another Fairway Field? (Part 2) [unpublished Master's thesis]: University of Michigan, Ann Arbor, 80 p.

Tipper, J.C., 1997, Modeling carbonate platform sedimentation—Lag comes naturally: Geology, v. 25, p. 495–498.

Tucker, M.E., 1991, Sequence stratigraphy of carbonate–evaporite basins: models and application to the Upper Permian (Zechstein) of northeast England and adjoining North Sea: Geological Society of London, Journal, v. 148, p. 1019–1036.

Vahrenkamp, V.C., Franseen, R.C.W.M., Grötsch, J., and Muñoz, P.J., 1993, Maracaibo platform (Aptian–Albian), northwestern Venezuela, *in* Simo, J.A., Scott, R.W., and Masse, J.-P., eds., Cretaceous Carbonate Platforms: American Association of Petroleum Geologists, Memoir 56, p. 25–33.

Valladres, I., Recio, C., and Lendínez, A., 1996, Sequence stratigraphy and stable isotopes ($\delta^{13}C$, $\delta^{18}O$) of the Late Cretaceous carbonate ramp of the western margin of the Iberian Chain (Soria, Spain): Sedimentology, v. 105, p. 11–28.

WARREN, J.K., 1989, Evaporite Sedimentology: Importance in Hydrocarbon Accumulation: Englewood Cliffs, New Jersey, Prentice Hall Advanced Reference Series, 285 p.

WARREN, J.K., 1991, Chapter 2, Sulfate dominated sea-marginal and platform evaporative settings: Sabkhas and salinas, mudflats and salterns, *in* Melvin, J.L., ed., Evaporites, Petroleum and Mineral Resources: Amsterdam, Elsevier, Developments in Sedimentology 50, p. 69–187.

WARREN, J.K., AND KENDALL, C.G.ST.C., 1985, Comparison of sequences formed in marine sabkha (subaerial) and salina (subaqueous) settings—modern and ancient: American Association of Petroleum Geologists, Bulletin, v. 69, p. 1013–1023.

WEISSERT, H., AND LINI, A., 1991, Ice age interludes during the time of Cretaceous greenhouse climate?, *in* Müller, D.W., Mckenzie, J.A., and Weissert, H., eds., Controversies in Modern Geology: New York, Academic Press, p. 173–191.

WIGLEY, T.M.L., AND RAPER, S.C.B., 1987, Thermal expansion of sea water associated with global warming: Nature, v. 330, p. 127–131.

WILBERT, W.P., 1976, Geology of the Sierra de la Paila, Coahuila, Mexico [unpublished Ph.D. thesis]: Tulane University, 187 p.

WILSON, J.L., 1967, Carbonate–evaporative cycles in the lower Duperow Formation of Williston Basin: Bulletin of Canadian Petroleum Geology, v. 15, p. 230–312.

WILSON, J.L., 1975, Carbonate Facies in Geologic History: New York, Springer-Verlag, 471 p.

WILSON, J.L., 1990, Basement structural controls on Mesozoic carbonate facies in northeastern Mexico—a review, *in* Tucker, M.E., Wilson, J.L., Crevello, P.D., Sarg, J.R., and Read, J.F., eds., Carbonate Platforms, Facies, Sequences and Evolution: International Association of Sedimentologists, Special Publication 9, p. 235–255.

WILSON, J.L., AND PIALLI, G., 1977, A Lower Cretaceous shelf margin in northern Mexico, *in* Bebout, D.G., and Loucks, R.G., eds., Cretaceous Carbonates of Texas and Mexico: The University of Texas, Bureau of Economic Geology, Report of Investigations no. 89, p. 302–323.

WILSON, J.L., AND WARD, W.C., 1993, Early Cretaceous carbonate platforms of northeastern and east-central Mexico, *in* Simo, J.A., Scott, R.W., and Masse, J.-P., eds., Cretaceous Carbonate Platforms: American Association of Petroleum Geologists, Memoir 56, p. 35–50.

WILSON, J.L., WARD, W.C., AND FINNERAN, J., 1984, A Field Guide to Upper Jurassic and Lower Cretaceous Carbonate Platform and Basin Systems, Monterrey–Saltillo Area, Northeast Mexico: SEPM, Gulf Coast Section, 76 p.

WILSON, M.A., AND PALMER, T.J., 1992, Hardgrounds and Hardground Faunas: University of Wales, Aberystwyth, Institute of Earth Studies, Publication 9, 131 p.

WINKER, C.D., AND BUFFLER, R.T., 1988, Paleogeographic evolution of early deep-water Gulf of Mexico and margins, Jurassic to Middle Cretaceous (Comanchean): American Association of Petroleum Geologists, Bulletin, v. 72, p. 318–346.

Received 1 November 1996; accepted 9 February 1998.